

A STUDY OF THE INTERSTELLAR MEDIUM IN NGC 185
AND OTHER EARLY-TYPE GALAXIES

By

DOUGLAS WILLIAM JOHNSON

A DISSERTATION PRESENTED TO THE GRADUATE COUNCIL OF
THE UNIVERSITY OF FLORIDA
IN PARTIAL FULFILLMENT OF THE REQUIREMENTS FOR THE
DEGREE OF DOCTOR OF PHILOSOPHY

UNIVERSITY OF FLORIDA

1980

to Maryfran

ACKNOWLEDGEMENTS

There are many people who have contributed invaluable resources and encouragement to me in the completion of the research for this dissertation. Although it is not possible to thank each one individually, there are some I would like to acknowledge in particular.

The Northeast Regional Data Center is acknowledged for providing a vigorous and stimulating computing environment. The operators of the 11 m NRAO telescope were very helpful in assisting me during my observing sessions and the assistance of Telescope Engineer Rick Howard was especially appreciated. I would also like to thank Dan McGuire for his assistance during my first observing session.

I thank my supervisory committee members, Dr. Stephen T. Gottesman, Dr. Thomas D. Carr, Dr. Kwan-Yu Chen, Dr. Gary Ihas, and Dr. William Weltner, for their attention and interest in my work.

I thank the Physics Department, and especially Dr. Richard Garrett, for the assistantships that have allowed me to pursue this course of study.

The Division of Sponsored Research is thanked for its Seed Money Grant Competition, providing financial support for Dr. Gottesman and me during the course of our investigations. The Graduate School's Supplementary Fellowship for 1979-80 was also greatly appreciated.

Finally, I wish to thank Steve Gottesman and his family for their efforts to make Maryfran's and my stay in Gainesville a wonderful time

in our lives. Steve's assistance and discussions with me (to say nothing of his witticisms) were above and beyond the call of duty.

I thank my parents, Bill and Mary Ann, for their support and love and good humor throughout the years. But I reserve perhaps my sincerest appreciation for Maryfran and the "kids" (Smokey, Phantom, Harpo, and Marble) for making it all worthwhile.

TABLE OF CONTENTS

	<u>Page</u>
ACKNOWLEDGEMENTS.	iii
ABSTRACT.	vii
CHAPTER	
I INTRODUCTION	1
The Nature of Early-Type Galaxies.	1
Galaxy Classifying Schemes	2
The Morphology of Elliptical Galaxies	3
The Morphology of Lenticular (S0) Galaxies.	6
The Formation and Evolution of Early-Type Galaxies	7
Formation	7
Mass Accretion.	11
Mass Loss Due to Stellar Evolution.	13
Stripping Mechanisms	15
Internally Driven Winds	15
Ram-Jet Stripping by an Intracluster Medium	18
Fate of Retained Gas	23
Supermassive Objects in the Nucleus	23
Cyclic Bursts of Star Formation	25
Continual Star Formation with a Skewed Initial Mass Function	27
Statement of Dissertation Problem.	29
II THE OBSERVATIONS	31
Carbon Monoxide Observations at Kitt Peak, AZ.	31
Telescope Description	31
Data Reduction Techniques	34
Data Presentation	35
Neutral Hydrogen Observations at Green Bank, WV.	36
Telescope Description	36
Data Reduction Techniques	38
III RESULTS.	39
Carbon Monoxide.	39
Positive Result in NGC 185.	39
Negative Results.	48
Neutral Hydrogen	51
IV DISCUSSION	68
NGC 185.	68
NGC 205.	84

	<u>Page</u>
Negative CO Results.	87
Neutral Hydrogen and NGC 185	93
V SUMMARY.	96
APPENDIX	
I CALIBRATION THEORY FOR CO OBSERVATIONS	100
II THE PHYSICS OF CO SPECTRAL LINE CALCULATIONS	105
III THE GEOMETRY IN AN INCLINED DISK	111
REFERENCES.	114
BIOGRAPHICAL SKETCH	120

Abstract of Dissertation Presented to the Graduate Council
of the University of Florida in Partial Fulfillment of the Requirements
for the Degree of Doctor of Philosophy

A STUDY OF THE INTERSTELLAR MEDIUM IN NGC 185
AND OTHER EARLY-TYPE GALAXIES

By

Douglas William Johnson

August 1980

Chairman: Stephen T. Gottesman
Major Department: Astronomy

The question of an interstellar medium in early-type galaxies is considered in light of the small amounts of gas detected as neutral hydrogen (HI). It is apparent that there is some method of removal or reprocessing that keeps the interstellar medium of early-type systems gas and dust free in spite of mass loss from normal stellar evolution.

A detection of ^{12}CO is presented for the dwarf elliptical system NGC 185. The mechanisms of line formation of the $J = 1 \rightarrow 0$ transition strongly imply that the emitting region is in a state of gravitational collapse. These observations are consistent with the observed dust content of the galaxy and its blue, presumably young stellar population. It is nearly certain that the galaxy is reprocessing its interstellar medium via star formation.

The radial velocity of the CO cloud can be combined with the velocity data for two planetary nebulae within the system to allow rough mass calculations. Coupling this information with luminosity data indicates that the mass-to-luminosity ratio of the nuclear regions (within 1 arcminute) is between 5 and 18, with a value near 8 being the most probable.

Observations of 10 other early-type systems are also presented and discussed. The negative results imply that the gas is either clumped and thus optically thick or has been removed from the system through a galactic wind, ram-jet stripping, or has been consumed by star formation.

The nature of the star formation must be somewhat different than that in our own galaxy. The high-mass end of the initial mass function for star formation would result in bluer colors than observed, the star formation must be skewed towards the low-mass stars to be effective yet unobserved. Theoretical arguments that this is possible are advanced, but more sensitive and highly resolved CO observations are necessary to observe directly this scale of star formation.

Neutral hydrogen observations of NGC 185 obtained with the NRAO 43 m telescope are presented and discussed. There is apparently low-level (20-40 mK) high-velocity hydrogen in the region of NGC 185. The most likely source of the material is the Magellanic Stream which terminates in this area. Superposed on this high-velocity material, at the same velocity, is an excess of about 5 mK of HI at the location of NGC 185. This was detected by using "off" spectra 1-2 beamwidths from the galaxy in the four cardinal directions. The observations cannot distinguish between an enhanced high-velocity feature projected onto the galaxy and genuine emission from the galaxy itself, but the results are very suggestive and should be followed up with observations of greater resolution.

CHAPTER I

INTRODUCTION

The Nature of Early-Type Galaxies

Since the discovery that the "spiral nebulae" were indeed island universes somewhat like our own, the effort to study, classify, and dissect them has been increasing with remarkable speed. In large measure this is due as much to the expansion of the accessible electromagnetic spectrum as to the increasing sensitivity of instruments within each spectral window.

The basic observational technique used for this dissertation, radio astronomy, dates from the 1932 observations of the Milky Way by Karl Jansky. The achievements with this relatively new technique have accumulated steadily over the past half century and it is now recognized as an invaluable tool in studying the universe and its contents.

One of the most attractive characteristics of radio astronomy is that it complements the endeavors of the oldest technique, optical astronomy. The analysis of visible light almost always entails objects with a temperature of at least 2000 K and the vast majority of objects this hot are stars. Radio astronomy, utilizing much less energetic quanta, is sensitive to objects of several hundred degrees or less. Typically this is primarily the interstellar gas that fills the space between the stars. There are important exceptions to this rule (synchrotron radiation, thermal bremsstrahlung, etc.) but it illustrates well the complementary nature of optical and radio astronomy.

Galaxy Classifying Schemes

Early studies of galaxies made it clear that the general morphology of these immense stellar systems allowed them to be grouped into a relatively small number of types. The most successful early venture was Hubble's "tuning fork" diagram published in 1936, and reproduced here in Figure 1. The spherical systems (E0) are at one end with progressively flatter (E1-E7) systems leading up to a split in the diagram. S0 galaxies (also called lenticular galaxies) occupy the vertex of the fork because Hubble believed that they were transitional systems. They contain prominent elliptical bulges as well as a conspicuous disk component. It is interesting to note that the nature of S0 galaxies is still being vigorously debated.

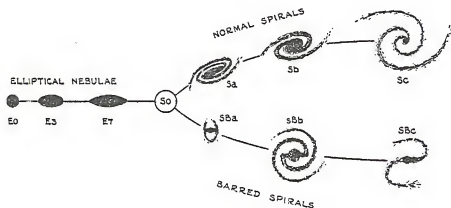


Figure 1. Hubble's "tuning fork" diagram of the classification of galaxies.

Forming the tines of the fork are two parallel sequences of spiral galaxies; one with a bar, the other without. The trend along the tines is from tightly wound spiral arms (Sa or SBa) to looser, more open arms at the end (Sb-Sc or SBb-SBc).

In addition to these major players in the drama, some 3% of all galaxies are irregular, possessing no dominant symmetrical structural features.

Many additions and modifications have been made to this initial classifying scheme (Hubble 1936, Morgan 1958 and 1979, de Vaucouleurs 1959, van den Bergh 1960a and b, Sandage 1961) but it has remained remarkably unchanged over the years. In large measure the modifications are to take into account the more extensive information available due to more sensitive equipment and increasing access to other spectral regions.

The following sections describe the elliptical and lenticular galaxies in more detail and lay the groundwork for the statement of the thesis problem in the final section of Chapter I. For historical reasons both elliptical and lenticular systems are commonly known as "early-type" galaxies.

The Morphology of Elliptical Galaxies

As the name implies, the elliptical galaxies are characterized by elliptical isophotes. The stellar population usually appears to be well-evolved with little or no interstellar gas or dust.

The degree of ellipticity E is defined to be $(a - b)/a$ (where a and b are the semi-major and semi-minor axes, respectively). The range observed is 0.0-0.7 (E0-E7) with E0-E1 the most common and decreasing in frequency at the flatter end of the range.

Taking into account the statistics of random projection on the sky (for we are viewing a two-dimensional projection of a three-dimensional object) it appears that the ellipticals are distributed normally about a mean of E3.6 ($e = 0.36$) with a dispersion of 0.11 (de Vaucouleurs 1977). It appears that true E0 and E5.5 (de Vaucouleurs contends that E5.5 is the flattest bona fide elliptical) are relatively rare.

The lack of flat systems, usually considered to be a dynamical effect caused by instabilities in thin disks, suggests that perhaps spiral density waves and the attendant star formation are suppressed in disks of sufficient thickness.

The origin of the flatness of elliptical systems has long been thought a natural consequence of rotation. The greater the rotational velocity, the greater the degree of flattening. This of course implies that the three-dimensional figure is an oblate ellipsoid (polar diameter smaller than the equatorial diameter).

In recent years several rotation curves of elliptical galaxies have been published (Bertola and Cappaccioli 1975, Illingworth 1977, Peterson 1978, Sargent et al. 1978, and Young et al. 1978a) which cast strong doubt on the validity of this simple approach. The small observed ratio of the maximum rotational velocity to the central dispersion velocity mitigates strongly against models which use isotropic velocity distributions and either oblate or prolate ellipsoids (Schechter and Gunn 1979). It appears necessary to use both anisotropic velocity distributions as well as rotation to account for the observed rotation curves (Binney 1978, Schechter and Gunn 1979).

The origin of the anisotropy is still not clear but the most likely source is remnant anisotropy from the collapse phase of the galaxies' formation.

A further difficulty in our understanding of elliptical galaxies is the existence of extreme population I ingredients in a significant number of systems. Specifically:

- OB clusters are observable in NGC 185 and 205 (Hodge 1963 and 1973)
- ionized gas is seen in the nuclei of at least 15% of all ellipticals (Osterbrock 1960 and 1962)
- neutral hydrogen has been detected in at least 8 elliptical systems:

NGC 1052 (Knapp et al. 1978b)
NGC 2974 (Bottinelli and Gouguenheim 1979b)
NGC 3904 (Bottinelli and Gouguenheim 1977b)
NGC 3962 (Bottinelli and Gouguenheim 1979a)
NGC 4105 (Bottinelli and Gouguenheim 1979b)
NGC 4278 (Gallagher et al. 1977)
NGC 4636 (Knapp et al. 1978a)
NGC 5846 (Bottinelli and Gouguenheim 1979b)

The presence of population I material is unusual for systems thought to have ended all star formation long ago. Some possible explanations are that the material was accreted relatively recently and thus it is not representative of an elliptical galaxy's normal evolution, or that through normal processes of stellar evolution the material was shed by the stars and is observable in various forms today.

The thrust of the foregoing observations is that, as a class, elliptical galaxies are not as well-understood as was earlier believed. The apparently relaxed stellar distribution is most likely not relaxed at all, but still contains velocity anisotropies which strongly influence the shape of the galaxy. It is disturbingly common for the smooth isophotes to be blemished with dust obscuration or some other

form of detectable population I material. . The CO detection described in Chapter III is another example of the incongruities present in elliptical systems.

The Morphology of Lenticular (SO) Galaxies

The lenticular systems, occupying the vertex of Hubble's tuning fork diagram, are as perplexing today as ever. The essential features of these galaxies are an elliptical bulge and a disk, both apparently composed of population II stars. The disks are devoid of spiral arms and the systems lack the obvious star formation proceeding in spiral galaxies.

Suggestions as to the origin of the lenticulars range from van den Bergh's proposal (1976b) that they are part of a complete sequence of gas-poor, "anemic" spirals parallel to the S and SB types to the more recent suggestion (Gunn and Gott 1972, Gisler 1979, and references therein) that they are normal spirals which have been stripped of their gas and dust by an interaction with an intracluster medium.

Much work has been done in recent years on these systems and some interesting observations have been reported. Neutral hydrogen observations by Balick et al. (1976) and a number of others place the lenticulars roughly midway between the Sa-SBa and E systems. This evidence supports the contention that they form another sequence of spirals much like the normal sequence, only gas-poor.

Further, Burstein (1979a,b,c) finds significant differences in the bulge-to-disk ratios of lenticulars and spirals, as well as "thick" disks in lenticulars and not spirals. These are structural

features that are difficult to affect by stripping mechanisms, thus supporting the parallel sequence hypothesis.

On the other hand, several people have investigated the spatial distribution of lenticular systems and find that they are concentrated within clusters, strongly suggesting that their current environment is crucial in their formation.

Regardless of the mechanism for the origin of the lenticular systems they have been included in this study because they share several significant properties with elliptical galaxies. The stellar populations appear quite similar and both have a lack of dust and gas within their interstellar media.

The Formation and Evolution of Early-Type Galaxies

Formation

The general outline of galaxy formation, and elliptical galaxy formation in particular, is understood only in its coarsest features. This section presents the scenario most widely agreed upon with emphasis on early-type systems. Significant gaps in the scenario are also noted with various suggestions that may, in the future, fill them.

In the study of galaxy formation one is inevitably forced to consider earlier epochs. In astronomy this can be done easily by observing more distant objects. The scale of the universe is such that the time radiation has taken to arrive here on earth represents a significant fraction of the object's existence. Continuing the effort to fainter (more distant) objects gradually crosses over to cosmology and the study of the origin of the universe.

Perhaps the most influential discovery in cosmology (and also bearing heavily on galaxy formation) has been the 2.7 K microwave background. The existence of nearly isotropic (see Cheng et al. 1979 for a discussion of a dipole anisotropy attributed to the earth's motion with respect to the background) homogeneous radiation with an apparent blackbody spectrum strongly constrains galaxy formation theories.

The cosmic background radiation is almost universally believed to be the remnant from the era of decoupling; the time when the universe had cooled enough to allow electrons and protons to recombine (about 3000 K). The effect of the formation of neutral hydrogen is to reduce drastically the opacity of the matter with respect to the radiation. Before recombination Thompson scattering of radiation off electrons coupled very strongly the matter with the radiation, they were kept in thermal equilibrium and cooled together. After decoupling the two components evolved essentially independently of one another and the 2.7 K background seen today is the remnant of the radiation component.

This forms the basis of the expectation that the early universe was homogeneous and isotropic. Actually one can only say that it is homogeneous and isotropic to at least the smallest scale observed, currently that means the background is smooth to within 1 mK on a scale of 7° (Smoot and Lubin 1979, see Sunyaev 1977 for a discussion of fluctuations).

The condensations that have eventually evolved into clusters of galaxies, galaxies and stars must have occurred during a later epoch. The nature of these perturbations is currently a topic of great interest. Several theories have been advanced to account for the processes by which the perturbations form and grow (see Gott 1977 and

Field 1975 for reviews) but it will likely be many years before any scenario is convincing and widely accepted.

Lynden-Bell (1967) proposed a theory in which the essential feature of a galaxy's structure is determined by the timescale of collapse from the background compared to the timescale of star formation. It can be well illustrated by considering the various structural components of our own galaxy.

Our galaxy consists of a disk of gas, dust, and relatively young stars. The gas and dust are continually undergoing star formation in which hot bright stars appear to be preferentially formed along spiral arms. Spiral shock phenomena may be important in regulating the star formation but regardless of the details there is a continuing processing of gas and dust into stars.

Also present is a spheroidal halo which contains little if any gas and dust. It is composed primarily of old stars and consequently evolves only as fast as the stars that compose it.

Lynden-Bell's theory suggests that these structural features are formed by varying rates of star formation occurring in the collapsing proto-galactic cloud. Various components form as it separates out from the cosmic expansion and begins to contract under its gravitational force.

The novel feature of the theory is that it can explain how the halo can relax in the time allowed. Essentially, the presence of a changing gravitational potential will permit relaxation of the stellar system much faster than would two-body encounters.

The stellar population of the halo is entirely old stars with no gas or dust. During the collapse the stars form and are then

dynamically independent of the remaining material. That is, the stars reflect the velocity dispersion of the cloud at the time of their formation.

As the material collapses further, star formation proceeds and eventually the gas becomes dense enough that damping forces become important. At this stage the gas gives up a great deal of kinetic energy to dissipative heating and, because of its angular momentum, settles down into a disk. Within this disk various processes, especially star formation, continue to the present giving spiral galaxies their distinctive optical appearance.

It takes only a minor modification of this scenario to produce an elliptical galaxy. If star formation has proceeded to completion before the dissipative effects can form a disk then a system will result which has no disk component and is essentially a halo population of stars. Models which can produce the observed luminosity profiles of ellipticals have been constructed (Larson and Tinsley 1974) and add credence to this basic concept.

Within this framework of galaxy formation many details are still to be worked out. As previously mentioned, the nature of the initial perturbations is not at all understood. Also the processes of fragmentation and collapse are poorly understood (Field 1975). There is even a question of whether gravitational instabilities or turbulence is responsible for the necessary condensations. Jones (1976) provides an excellent review of these and other problems in the study of galaxy formation.

Since the early star formation was apparently so efficient as to consume all the primordial gas, one might not expect any continuing

star formation in elliptical galaxies. It will be shown, however, that other processes operate which alter this simple picture and lead to radically different expectations. The most important effects are mass loss from the normal evolutionary processes of the stellar population and perhaps accretion of extragalactic material; both are discussed in the following sections.

Mass Accretion

The contention that early-type galaxies, ellipticals in particular, accrete material is relatively new. The motivation is to explain the cD galaxies (giant ellipticals usually located in the center of rich clusters and described by Bautz and Morgan 1970) that are often strong radio sources. The accretion described here is full scale cannibalism of other galaxies during close encounters (Ostriker and Tremaine 1975, White 1976, Ostriker and Hausman 1977, Hausman and Ostriker 1978).

The idea can be linked to cluster types as described by Bautz and Morgan (1970) and Oemler (1974). This cluster classification scheme ranks the clusters based on their richness. Observationally it is found that the densest clusters (Type I in the notation of Bautz and Morgan 1970) often contain giant elliptical galaxies near their center. Further, the cD galaxies are often radio sources that are widely suspected to be caused by material falling into a massive object. There are several other pieces of circumstantial evidence that indicate that this process may indeed be significant in the evolution of elliptical galaxies (see Ostriker 1977 and Hausman and Ostriker 1978 for details).

A more moderate form of mass accretion is suggested by several authors (Bottinelli and Gouguenheim 1977a, Gallagher et al. 1977, and Knapp, Kerr, and Williams 1978c) to explain the inclined disk of NGC 4278. The differing directions of the angular momentum of the stellar component of the galaxy and the neutral hydrogen make an internal origin of the matter difficult to believe.

A similar situation occurs in NGC 1052 (Knapp, Faber, and Gallagher 1978a, Fosbury et al. 1978, Reif, Mebold, and Goss 1978) and the accretion of an intergalactic HI cloud is suggested. The major objection to this hypothesis is the lack of sufficiently massive clouds available for accretion.

The results of Mathewson et al. (1975) purporting to find HI clouds in the Sculptor group have been disputed by Haynes and Roberts (1979). The latter group contend that the material is a portion of the Magellanic Stream. Further, Lo and Sargent (1979) have searched nearby groups for detached HI clouds and find none more massive than $\sim 4 \times 10^7 M_{\odot}$.

A number of other authors have examined clusters of galaxies for HI emission (Haynes et al. 1978, Baan et al. 1978) while others have examined the line of sight to quasars for HI absorption (Roberts and Steigerwald 1977, Shostak 1978). No isolated HI clouds are seen in emission in the clusters and the HI absorption measurements show that large clouds of neutral hydrogen are almost never seen outside galaxies.

Thus it appears difficult to reconcile the several times $10^8 M_{\odot}$ of HI found in NGC 4278 and 1052 with the dearth of sufficiently massive candidates for accretion. Silk and Norman (1979) propose an

alternative hypothesis, the accretion of gas-rich dwarf galaxies. They find that the gas component of the dwarfs will lose energy through dissipation and fall to the central regions of the accreting galaxy. The infalling gas, depending on the individual cloud mass, may either form stars or continue to fall into the nucleus where it may fuel a radio source. The stars will also be incorporated into the accreting galaxy but with less visible effects.

Silk and Norman (1979) also consider the interaction of a Mathews and Baker (1971) type wind and the infalling material. If the amount of this material is sufficiently large the resulting supernovae (from the high-mass stars formed) will help in driving the galactic wind. However, an enhanced wind has the effect of inhibiting mass infall and the process slows itself. The net effect may be for star formation to proceed in cyclical bursts--a notion also suggested by van den Bergh (1975) in a somewhat different context.

Both of the mass accretion processes described so far deal with normal or giant cD elliptical galaxies. In order to be effective in capturing and assimilating other systems the accreting galaxy must be large. The evolutionary mechanism discussed in the following section, mass loss from stellar evolution, operates in all systems. This includes the dwarf ellipticals NGC 185 and 205 considered in greater detail in Chapter III.

Mass Loss Due to Stellar Evolution

It has recently been appreciated that the normal evolution of stars in an early-type galaxy will be a source of interstellar material.

Small mass stars have stellar winds, Mira variables are known to eject mass during certain stages, Type I supernovae occur in population II stars, and planetary nebulae have been observed in early-type galaxies of the local group.

The calculation of the contribution by stellar evolution to the interstellar medium (ISM) of early-type galaxies depends more on theoretical estimates than observational evidence. To date, the most important observational evidence is the detection of planetary nebulae in nearby dwarf ellipticals (including NGC 185) by Ford and Jenner (1975). Considering the uncertainties in the observations, the observed planetary birthrate of $\geq 0.012 \text{ yr}^{-1} (10^9 L_{\odot})^{-1}$ agrees well with Larson and Tinsley's (1974) estimate of $0.05 \text{ yr}^{-1} (10^9 L_{\odot})^{-1}$.

Following the reasoning of Faber and Gallagher (1976) and adopting a mass per planetary of $0.2 M_{\odot}$ results in a mass loss rate of $0.010 \text{ yr}^{-1} (10^9 L_{\odot})^{-1}$ from planetaries. Consideration of Mira-type variables leads to a final assumed mass ejection rate of $0.015 \text{ yr}^{-1} (10^9 L_{\odot})^{-1}$.

The conservative nature of this calculation is apparent when one considers that the present mass loss rate is certainly lower than that of earlier epochs. This is primarily because any high-mass stars would have evolved quickly and cycled their mass back to the ISM early in the galaxy's evolution.

Further, the contribution of mass from Type I supernovae (apparently confined to population II stars, Tammann 1974) and Type II supernovae (massive progenitors) earlier in the galaxy's evolution have been ignored. Even this conservative approach leads to contradictions in the ISM of early-type galaxies after 10^9 - 10^{10} years (Faber and Gallagher 1976).

Stripping Mechanisms

The various efforts to determine how interstellar material shed by stars can be removed from early-type systems can be divided into two classes. The first is an internally driven "galactic wind" and second is ram-jet stripping by an intracluster medium. Both of these processes will be discussed in the following sections.

Internally Driven Winds

The possibility of a galactic wind driven by an internally driven energy source was suggested by Johnson and Axford (1971) and considered more quantitatively by Mathews and Baker (1971). In essence the mechanism operates by coupling the energy from Type I supernovae to the general interstellar medium. The addition of this high-energy (8×10^9 K) low-mass component significantly heats the interstellar material to a high enough temperature to escape from the system by evaporation. A later study by Coleman and Worden (1977) shows that the energy released by flare stars is by itself enough to drive a galactic wind of this type.

The parameters that are most important in the establishment and maintenance of a galactic wind are the Type I supernovae rate, the energy output from each supernova, the efficiency of the coupling of the supernova's energy to the ISM, and the amount of "pre-heating" of the ISM by the velocity dispersion within the galaxy. Each of these quantities are known to probably a factor of 2 at best and in certain instances various authors disagree by factors of 10 or more.

For example, Mathews and Baker (1971) assume a coupling efficiency between the expanding supernova shell and the ISM of 1; that is, all the kinetic energy of the supernova is converted into thermal energy of the ISM. Gisler (1976) takes exception to this number and notes that Larson (1974) uses an efficiency of 0.1. Given the various uncertainties it appears that while a galactic wind will most likely prevail in some instances, perhaps even a majority of elliptical galaxies, there are cases in which it simply does not operate.

Indeed, Mathews and Baker (1971) find solutions in which a wind is not supported and the material collapses to the center of the system. They further propose that the hot, ionized gas will only be able to form massive objects, thus linking the lack of a galactic wind to the formation of radio sources in early-type galaxies.

Again, Gisler (1976) points out an inconsistency in this line of reasoning. From observations one finds that strong radio sources were more common in earlier epochs. Gisler notes that the earlier stellar content of ellipticals is more likely to produce supernova. This follows from the observation that only Type I supernovae occur in population II (old) stars and the precursors are probably low mass stars (Tammann 1974). In the earlier stages of an elliptical's life the supernova rate can only be augmented by Type II supernovae (whose progenitors are young, massive stars). In addition it is at the earlier epochs that the galaxy will not have had time to collect a significant amount of gas from the evolution of its stellar component. For these two reasons it would appear that the ellipticals are better able to support a galactic wind at earlier epochs--just the period when the greatest fraction must also be radio sources.

Faber and Gallagher (1976) have considered the problem of a galactic wind from a slightly different approach. Since the initial heating of the ISM is through collision of the gas clouds shed by stars in the process of normal evolution, the velocity dispersion of the stars can be used as an indicator of the stellar equivalent temperature, T_s . From Mathews and Baker (1971) $T_s = v_s^2 m_H / 6k$ where v_s is the stellar dispersion velocity and m_H is the mass of the proton, and k is Boltzmann's constant. Along with the condition that the supernova-induced rise in temperature must roughly double the kinetic energy of the gas to remove it from the system to infinity, one finds

$$\alpha_{sn} T_{sn} \geq \alpha_s T_s \quad (1)$$

where α_{sn} and α_s are the specific rates of mass injection by supernovae and stars, respectively, T_{sn} and T_s are the equivalent temperatures of the supernovae and the stars.

Using the values quoted in Faber and Gallagher (1976) $\alpha_s = 5 \times 10^{-20} \text{ sec}^{-1}$ and $\alpha_{sn} T_{sn} = 1.6 \times 10^{-12} \text{ K sec}^{-1}$ yields $T_s = 3.7 \times 10^7 \text{ K}$ or $v_s \leq 1260 \text{ km/sec}$. The line-of-sight velocity dispersion is $\leq 1260/\sqrt{3} = 730 \text{ km/sec}$ (assuming 3 dimensional isotropy of the velocity dispersion); which exceeds by a factor of two the largest velocity dispersions measured (Faber and Jackson 1975).

This calculation would make it appear that virtually all elliptical systems should have a galactic wind scouring the ISM of any material. However, Gisler (1976) recomputes this same quantity, taking into account the 0.1 efficiency of energy coupling found by Larson (1974), and finds that the maximum velocity dispersion that will still allow the supernovae to double the energy is about 200 km/sec, a number comparable to the observed velocity dispersions. In other words,

if a galaxy has a velocity dispersion greater than 200 km/sec then the supernovae contribution will not be able to double the kinetic energy of the ISM and a galactic wind cannot be established.

Even more damaging to the galactic wind hypothesis is the detection of HI in any elliptical. In order for the wind to operate the ISM must be hot ($\sim 10^7$ K). All of the gas in a galaxy would thus be ionized and according to Mathews and Baker (1971) quite unobservable by present techniques.

A final argument against the universal existence of galactic winds is that if all other conditions were the same, one would expect the more spherical systems to be better able to support a galactic wind. The reasoning is that the spherical systems have less surface area per unit volume through which to radiate excess energy, keeping the ISM as hot as possible.

Contradicting this expectation, the neutral hydrogen observations of 8 elliptical systems show detections significantly skewed towards the more spherical galaxies. The systems detected in neutral hydrogen have the following classifications: 2-E0, 2-E1, 1-E2, 1-E3, 2-E4. Conspicuously absent are the flatter systems that one would expect to be better able to radiate energy away and thus retain their ISM.

Ram-Jet Stripping by an Intracluster Medium

The proposal that ram-jet stripping of an ISM could be significant in the evolution of a system was treated first by Gunn and Gott (1972). Later, more sophisticated treatments by Tarter (1975), Gisler (1976), and Lea and De Young (1976) all support the notion that stripping can be an effective process.

The thrust of much work in this area has been to determine if S0s can be formed by stripping spiral galaxies of their gas and dust (Gisler 1979). This would quench star formation and significantly change the optical appearance of the galaxy.

Another development that has spurred interest in the interaction of an ISM with an intergalactic medium (IGM) is the discovery of head-tail radio galaxies. The most straightforward explanation of this phenomenon being just such an interaction.

In spite of the varied motivations for these studies many of the numerical simulations are directly applicable to the analysis of an elliptical system passing through an IGM.

The primary results of these studies are to confirm that under appropriate conditions there is an effective sweeping out of material from the galaxy. The procedures and model parameters used to arrive at this conclusion vary substantially for the different experiments, all agree however, that some material tightly bound near the nucleus may be retained. Gisler (1979) explores the situation further and finds that the rate of gas replenishment is important, possibly stopping the stripping effect entirely if it is high enough.

In spite of this it appears that stripping can be at least partially effective over a broad range of galaxy velocities and IGM densities. This finding agrees well with the observation that a large fraction of galaxies in rich clusters are S0s and ellipticals (Oemler 1974, 1977).

It would seem also that the evidence of a positive correlation between X-ray luminosity of clusters (presumably from a hot intracluster component) and S0/spiral ratios (Tytler and Vidal 1978) argues strongly

that the cluster environment does indeed have a significant influence on the structure and evolution of its component galaxies.

An evolutionary effect may also have been observed by Butcher and Oemler (1978). Their study found that a rich cluster observed at a redshift of 0.4 contains many more blue galaxies than a similar rich cluster observed in the current epoch. Their conclusion is that as late as 4×10^9 years ago the galaxies in this cluster had not yet been stripped of their ISM. They were consequently undergoing at least moderate star formation, thus producing the blue colors observed.

One further piece of evidence that fits in quite well with the general hypothesis of ram-jet stripping is the common coincidence of a strong radio galaxy at the center of a dense cluster (McHardy 1974, Guthrie 1974, and Riley 1975). The argument in this case is that the central galaxies have a small velocity with respect to the intra-cluster medium and will be more likely to retain gas shed by its stellar population. The material collapses to the center of the galaxy, apparently forming a massive object and producing the observed radio source.

In view of the variety of indications that imply a substantial interaction between an ISM and an intracluster medium it seems clear that environmental factors can be important in the evolution and structure of galaxies in clusters. But in the particular case of the detected ellipticals NGC 4278 and 4636 there is reason to believe the IGM is unimportant.

These are the only two galaxies which have an HI distribution that is extended enough to map. In both instances the HI distribution appears to be considerably wider than the photometric diameter of the

system (Knapp et al. 1978a, Bottinelli and Gouguenheim 1979a). More importantly, the distributions appear to be reasonably symmetric, a condition difficult to reconcile with stripping or partial stripping by an intracluster medium. This discrepancy is pursued further in Chapter IV.

Other evidence that ram-jet stripping may not be as effective as the numerical analyses indicate is found in the Hercules cluster, a rather loose cluster composed almost entirely of spiral galaxies. The inconsistency is that it is also an X-ray source. Our current understanding of cluster X-ray sources necessitates a hot ($\sim 10^7$ K) intracluster medium as the origin of the radiation. How the Hercules galaxies have remained spirals and not been stripped is not understood within the framework of current research. Even more perplexing is the origin of the intracluster gas, it is usually thought to have been the gas removed from the galaxies.

A recent statistical study of cluster morphology by Gisler (1980) shows that the anticipated presence of Sc galaxies in clusters is not found. The Sc galaxies are expected to be highly resistant to having their ISM swept because they have a high rate of gas replenishment (Gisler 1979). The apparent underabundance in rich clusters indicates that ram-jet stripping cannot be the dominant mode of S0 production.

Dressler (1980) comes to similar conclusion based on a study of the morphology of the galaxies in 55 rich clusters. He finds a significant number of S0 systems in clusters which have too low a density to accomplish any stripping. Further, the study finds a difference between the bulge-to-disk ratios of spirals and S0s as well as a tendency towards thicker disks in S0 systems. From these

observations Dressler (1980) concludes that spirals do not evolve into S0s. He concludes that the galaxy types are affected more by the initial conditions at the time of their formation than by environmental factors such as ram-jet stripping.

Fate of Retained Gas

Supermassive Objects in the Nucleus

Mathews and Baker (1971) suggested that if their galactic wind should fail, the gas in the system would fall to the nucleus in an ionized state. They further argue that the Jeans radius

$$R_J = \left[\frac{\pi k T}{16 \mu M G (\rho + \rho_*)} \right]^{\frac{1}{2}} \quad (2)$$

where T is the temperature, μ is the molecular mass, G is the gravitational constant, ρ and ρ_* are the densities of the gas and stars, respectively, and k is Boltzmann's constant is determined primarily by the stellar density. That is, as the gas collapses it responds to the gravitational field of the stars. This will continue until the gas becomes more dense than the stellar component. The gas is dense and collapsing quickly at this stage and Mathews and Baker suggest that there may not be enough time for fragmentation to take place. The collapsing material then forms a massive object rather than fragmenting and forming stars with a normal distribution of masses.

Another argument for supermassive objects is the observation that cD galaxies with radio emission are often located in the center of dense, rich clusters. The evidence is largely circumstantial but if ram-jet stripping is important in the evolution of ellipticals then it follows that the central members of a cluster will be least affected by this mechanism. Of course the step from ineffective ram-jet stripping to a supermassive object in the galaxy's nucleus is by no means secure. It rests on the assumption that the retained material

either forms the supermassive object or at least provides fuel for the radio emission.

These arguments actually rest on much firmer ground due to recent work on the velocity dispersions and light distributions within the nuclei of supergiant cD galaxies found in the centers of rich clusters. Young et al. (1978b) obtained luminosity profiles of the supergiant elliptical NGC 4486 (M87) which, when examined with the velocity dispersions determined by Sargent et al. (1978), show that the nucleus contains a massive dark object. The nature of the dark object cannot yet uniquely be determined, but it must contain $5 \times 10^9 M_{\odot}$ of material and have a radius less than or equal to 100 parsecs (pc). Young et al. also determined that the mass-to-luminosity ratio must be greater than 60. Several possibilities are advanced but Young et al. find the most plausible to be a massive black hole of $5 \times 10^9 M_{\odot}$. The attraction of this hypothesis is that the $10^{42} \text{ erg sec}^{-1}$ energy output of NGC 4486 can be explained by supposing a mass infall of about $10^{-2} M_{\odot} \text{ yr}^{-1}$ with only a 0.002 conversion efficiency into radiation.

De Vaucouleurs and Nieto (1979) confirmed the results of the Young et al. (1978b) study and found essentially similar results for the dark mass at the nucleus. The earlier results were obtained with a CCD (charge-coupled device) camera, while the work by de Vaucouleurs and Nieto was with more conventional photographic and photoelectric photometry.

Young et al. (1979) also examined the luminosity profiles of NGC 4874, 4889, and 6251 and found that only NGC 6251 requires a supermassive object at its center to fit the data. Further, only NGC 6251 is a radio source amongst the three.

It appears from these observations that there may be a correlation between radio galaxies in the center of clusters and anomalous nuclei. Since current understanding of radio sources usually involves massive objects (which can also explain the anomalous nuclei) the circumstantial connection between a lack of ram-jet stripping and a supermassive object in a galaxy's nucleus is established.

However, within this scenario it is quite unclear whether the retained gas actually formed the massive object or just fuels it. The possibility that the galaxy formed with a massive nucleus cannot be overlooked; indeed, one of the central questions yet to be answered is how important are the initial conditions under which the galaxy formed.

Cyclic Bursts of Star Formation

The contention that the star formation rate in an elliptical or S0 galaxy is strongly dependent on time gains credibility only recently. Van den Bergh (1975) cites several examples of elliptical galaxies experiencing anomalously vigorous star formation.

NGC 5128 (also known as the radio source Centaurus A) has recently been shown by van den Bergh (1976a) to be undergoing very active star formation along and interior to its prominent equatorial dust band. He also suggests that the source of the unusual dust and gas in the system is stellar debris shed by the stars. The galaxy is apparently a rare field elliptical. It does not belong to a rich cluster and presumably lacks any ram-jet stripping which may exist in such an environment.

A strong argument against this hypothesis is the finding by Graham (1979) that the old stellar population rotates much slower than

the equatorial band of dust and gas. This is difficult to reconcile with the interstellar material originating with the stars. Most other researchers in the field tend toward the explanation that the system may actually be a collision between a gas cloud or small galaxy and an elliptical (Graham 1979). Thus the relevance of NGC 5128 to elliptical galaxy evolution cannot be assessed until these questions are answered.

Van den Bergh (1975) has also suggested that NGC 1275 is an example of an elliptical galaxy caught in a burst of star formation. The underlying stellar distribution in the system is elliptical and the galaxy is located near the center of the Perseus cluster. The small velocity difference between the cluster's mean velocity and that of the galaxy again suggests inefficient ram-jet stripping.

However, more recent work on the system (Kent and Sargent 1979, Rubin et al. 1977) indicate that this is a collision between a foreground spiral system and NGC 1275 in progress. Thus both NGC 5128 and 1275 may be atypical as far as early-type galaxies are concerned.

However, these two examples support the view that a massive ($\sim 10^9 M_{\odot}$) influx of material over a relatively short time period results in vigorous star formation. As both these systems are also radio sources, one could argue that another effect of the mass accretion is to either form, or fuel a previously existing, massive object in the nucleus, producing the radio source.

Further support for this hypothesis, although not in an early-type system, may be found in the M81-82 system. The interaction between these galaxies seems to be resulting in a substantial mass infall to M82 (Gottesman and Weliachew 1977, Killian 1978). It is likely that

the infall is connected with the peculiar structure of M82 and its vigorous star formation.

On a gentler scale there are several examples of star formation in dwarf ellipticals in the local group. NGC 185 and 205 both contain dust patches and a sprinkling of blue, presumably young stars. The CO observations described in Chapter III show that the star formation is probably continuing in NGC 185. NGC 205 is a close companion of M31 and it may be argued that an interaction is taking place, although HI maps of the region do not support this idea. Regardless, NGC 185 is considerably further from M31 and an interaction does not appear likely (see the HI observations presented in Chapter III concerning this possibility).

Consequently, it appears that these two dwarf ellipticals are reprocessing their ISM back into stars. The most likely source of the material is the normal products of evolution of stars. Large scale interactions are apparently not supported by the HI observations of the galaxies.

The more sedate pace of star formation, and various arguments suggesting an initial mass function for the stars shifted to lower masses, are examined in the following section.

Continual Star Formation with a Skewed Initial Mass Function

A third fate that may befall gas retained in early-type systems is star formation. The most stringent requirements on the nature of this star formation are set by the observations of the colors or early-type galaxies (see Larson and Tinsley 1978 for a discussion and earlier references).

Larson and Tinsley (1974) have calculated models for elliptical galaxies with star formation rates, continuing to the present, capable of consuming the gas shed by other stars. While the integrated colors of the models are consistent with observed galaxies, the expected gradient of increasingly blue colors in the nucleus is not widely observed. The most obvious drawback in their modeling is the use of an initial mass function (IMF) which is fairly rich in hot stars.

As Faber and Gallagher (1976) comment "Since we have no a priori knowledge of the IMF in ellipticals, star formation might conceivably be confined to stars of small mass and low luminosity" (p. 370). They go on to point out that the star formation must proceed efficiently since very little, if any, interstellar material is seen in most elliptical galaxies.

There is, however, observational evidence for star formation with an anomalous IMF. Van den Bergh (1976c) suggests that an IMF deficient in high mass stars is the most likely explanation for the lack of HII regions in the Sa galaxy NGC 4594 (M104). Knots of young, blue stars are observed near the prominent dust lanes. Normal, massive O and B stars would form prominent HII regions under such conditions. Further, this galaxy was not detected by Gallagher et al. (1975) in HI even though a normal dust-to-gas ratio indicates it should have been easily seen. Van den Bergh suggests that the lack of HI is due to its being converted into molecular hydrogen, thus escaping detection.

On theoretical ground also, an IMF skewed away from massive stars may be expected. Jura (1977) finds that one effect of reduced heating of interstellar clouds (expected in elliptical galaxies) is to allow clouds with much smaller masses to become gravitationally unstable

and collapse. Indeed, he finds that the critical mass for collapse under such conditions is less than $10 M_{\odot}$. Because of fragmentation the result of the collapse of a $10 M_{\odot}$ cloud will almost certainly be a number of small mass stars rather than one $10 M_{\odot}$ star.

Thus while no compelling reason can be advanced to accept star formation with a skewed IMF, the possibility cannot be rejected either. The main intention of this dissertation as outlined in the following section is to examine this possibility to determine if it is a significant process in the evolution of early-type galaxies.

Statement of the Dissertation Problem

From the previous sections it is clear that our understanding of early-type galaxies is incomplete. There are a large number of interesting ideas concerning their formation and evolution, but as usual, insufficient data are available to assess adequately their importance.

The primary goal of the observations presented and discussed in this dissertation is to investigate the significance of star formation in the evolution of early-type galaxies. The results of this study are most directly applicable to the recycling of material by star formation in an environment much different than our own galaxy. The results also bear on other settings in which the star formation is poorly understood.

It is not overstating the current situation to say that we only have a dim view of how star formation occurs in our own galaxy, and an even dimmer view of the process in drastically different environments. Faber and Gallagher (1976) argue that possible star formation in

early-type systems must be very efficient; if so, it may be generically related to the star formation that occurred as the galaxy collapsed originally. Judging from the lack of primordial material observed, that process was also very efficient.

This work is also of importance in the formation and continued activity of radio sources in early-type galaxies. From the available information it seems that radio sources and star formation are competing for the same interstellar debris in a galaxy. If one is very successful, it may be at the expense of the other.

All of this is not to say that galactic winds and ram-jet stripping never occur, simply that all possibilities need to be analyzed and evaluated to determine their relative importance in the overall scheme of galaxy evolution.

CHAPTER II

THE OBSERVATIONS

This chapter presents the data acquisition and handling procedures used for the work described in this dissertation. The instruments used are described giving particular attention to the equipment and techniques which aided this work immensely. The method of data presentation is also explained.

Carbon Monoxide Observations at Kitt Peak, AZ

Telescope Description

The observations searching for the 2.6 mm transition of $^{12}\text{C}^{16}\text{O}$ were made at the National Radio Astronomy Observatory (NRAO) Millimeter Wave Telescope¹ at Kitt Peak, AZ. The telescope is an 11 m paraboloid which can be driven in altitude and azimuth. Tracking of celestial objects, data acquisition, monitoring of system status, as well as initial data reduction is handled by an on-line PDP 11/40 computer.

The observations were taken during three separate observing sessions

December 23-26, 1977
July 7-9, 1978
December 10-16, 1979

¹The National Radio Astronomy Observatory is operated by Associated Universities, Inc., under contract with the National Science Foundation.

The cooled mixer cassegrain receiver operating at the 115.2712 GHz assumed rest frequency of the $J = 1 \rightarrow 0$ CO transition was used for all observations. The halfpower beam width at this frequency is about 65".

Pointing for the telescope is initially determined by the observatory personnel. Pointing correction data are taken in all parts of the sky on bright mm point sources. Analytic functions are then fitted to the data, interpolated over regions with few data points. The observer then checks these corrections by making five-point maps of bright sources, usually the planets. Rarely are the corrections more than 5 arcseconds at this stage.

However, the 1979 observations were hindered by large errors in regions far from the celestial equator due to a lack of adequate data for the fitting equations. This problem is discussed further in Chapter III.

Nominally, the sky signal is separated into two linearly polarized orthogonal components. In practice the system operated with only one polarization, except during the 1979 observations when both channels were available. These two signals are then fed to two Schottky-barrier mixer diodes. Also fed to the mixer is the local oscillator (LO) signal via a tunable injection cavity. This process of mixing two frequencies to get a third (usually the difference of the two) is known as heterodyning. The first intermediate frequency (IF) signal emerges at 4750 MHz and is amplified by a pair of low-noise parametric amplifiers. All of the previous equipment is enclosed in a dewar cooled to 15 K.

Once outside the dewar the 4750 MHz first IF is amplified again by room temperature transistor amplifiers. The signal is heterodyned further at this point to 1328 MHz.

A third and final mixer produces a 150 MHz third IF which is detected by two banks of 256 square-law detectors. One has a choice of filter widths for the filter banks; our observations always used either the 0.5 or 1.0 MHz (per channel) banks, corresponding to 1.3 and 2.6 km/sec velocity resolution, respectively. The December 1977 and July 1978 observations were made with only a single polarization operating, so the separate channels were actually the same signal and could not be averaged to reduce noise. Consequently the 0.5 MHz (1.3 km/sec) and 1.0 MHz (2.6 km/sec) filter banks were both used. At the time of the December 1979 observations the receiver operated in a proper two-channel mode with two independent IFs. Both were fed to 1 MHz filterbanks since they could now be added with a resultant decrease in noise.

Calibration was accomplished by alternately observing blank sky and an ambient temperature microwave absorber. Details of the calibration procedure are explained in Appendix I.

As a result of the calibration procedure one obtains the corrected antenna temperature of the source

$$T_A^* = \eta_f (1 - e^{-\tau}) [J(\nu_s, T_E) - J(\nu_s, T_{bg})] \quad (1)$$

where the explanations for the symbols are found in Appendix I. Note that there are three unknowns (η_f , τ , T_E) related to the particular source being observed; these cannot be determined without additional information. For extragalactic work one can make estimates for τ and T_E based on galactic studies and then calculate η_f . The

errors are large in this approach and they give only a general idea of the nature of the molecular cloud being observed.

Data Reduction Techniques

Each spectrum consists of two channels of 256 points each. For December 1977 and July 1978 only one polarization was available and it was detected in both the 256 MHz wide filter bank as well as the 128 MHz wide filter bank. The December 1979 observations took advantage of the two orthogonal polarizations then available and detected them separately in two 256 MHz filter banks. At the rest frequency of the $J = 1 \rightarrow 0$ transition of ^{12}CO the 1 MHz resolution corresponds to 2.6 km/sec.

The on-site PDP 11/40 computer writes the data for each spectrum (typically representing 5-10 minutes of observing) on disk. Real time analysis can be done at the telescope and allows the observing time to be optimally used. At the completion of the observing session the disk is copied onto a binary coded tape.

The next step in the processing is to rewrite the tape with the IBM 360 computer at the NRAO in Charlottesville, VA, to put the information into an IBM-compatible format. This is entirely a translation and no analyses are performed.

The final reduction is done at the University of Florida using the resources of the Northeast Regional Data Center. Each spectrum is examined for an unusually high root-mean-square deviation; all of the offending spectra are rejected. The baselines are then examined and if a polynomial of more than first degree is required to fit the baseline, the spectrum is discarded.

At this stage of the reduction process each point of the spectrum is examined to see if it is greater than five times the standard deviation for that spectrum. If it is, and the adjacent points are not, the point is replaced with the mean of the two adjacent points. This procedure is used to remove interference that involves only a single channel; multichannel filter banks are particularly susceptible to this type of interference.

Each spectrum is then weighted by the inverse square of its standard deviation and combined with all other spectra on the same source.

A preliminary first order baseline is fit and subtracted and the resulting spectrum is examined for possible features. If any are apparent the channels involved are eliminated from the baseline fitting procedure and a new first order baseline is calculated and subtracted.

The resulting spectrum represents the best data on a given source. Various smoothing functions can be applied; the most common for this work has been smoothing with a rectangular function of about the same width as the suspected spectral feature. The effect of this is to maximize the signal-to-noise ratio at the expense of velocity resolution.

The basic format of each spectrum presented is explained in Figure 2.

Data Presentation

The data are displayed with antenna temperature as the ordinate and velocity along the abscissa. Strictly speaking the abscissa

represents frequency, but since the frequency of the molecular transition is already known the axis is calibrated in km/sec using the following relation

$$v_s = \left\{ \left[\frac{v_r - v_{obs}}{v_r} \right] c - v_f \right\} / (1 - v_f/c) \quad (2)$$

where v_s is the center velocity of the observed band, v_f is the velocity of the source (corrected for the earth's rotation and revolution, i.e. heliocentric), v_r is the rest frequency of the spectral features, and v_{obs} is the observed frequency.

The ordinate, corrected antenna temperature (T_A^*), is found by calibration as described in Appendix I. The unit is Kelvins (K), and it is related to the flux density (S) by the following equation

$$S = 2 k \eta_L T_A^* / A_e \quad (3)$$

where η_L is the antenna efficiency due to the loss of elements (spillover, blockage, and ohmic losses in the antenna), A_e is the effective area of the antenna, and k is Boltzmann's constant.

Neutral Hydrogen Observations at Green Bank, WV

Telescope Description

The neutral hydrogen observations were made with the NRAO 43 m radio telescope at Green Bank, West Virginia. The telescope is an equatorially mounted instrument completely under computer control. The observations were taken during one session from July 13 to July 23, 1978.

The 21 cm cooled cassegrain receiver was used for all data acquisition. The system has two channels provided by linearly polarized, orthogonal feeds. After initial amplification by a cooled upconverter amplifier the signal is heterodyned and amplified through various stages in much the same fashion as the process described for the 11 m telescope at Kitt Peak. Typical system temperatures for the 43 m system were 50-60 K.

The standard NRAO "back end" uses a 150 MHz IF which is fed into a Model II autocorrelator spectrometer. The IF signal is autocorrelated and the resulting autocorrelation function is Fourier transformed to produce the power spectrum. The formation of the spectrum using autocorrelation techniques is described in more detail by Blackman and Tukey (1958) and Cooper (1976).

A 10 MHz bandwidth was chosen for all observations to provide an adequate baseline. Also in the interest of baseline stability a position-switched mode of observing was adopted. Ten minutes of data are taken at the "off" position followed by 10 minutes at the "on" position. The final spectrum is found by differencing the two spectra thus acquired.

A number of "off" positions were used in an effort to deduce the distribution of HI in the region around NGC 185. The majority of the data were taken either with an "off" 16^m to the west or as a five-point map. The arrangement for the five-point map is with the "on" at the center and "offs" taken successively to west, east, south, and north at a distance of either 48' or 24'. The half-power beam-width at 21 cm is about 20.5'.

Data Reduction Techniques

The output of the autocorrelator is two 192 channel spectra, each being linearly polarized but orthogonal to the other. The spectra are recorded by an on-line disk drive which can also be accessed by the on-line reduction computer. In operation, the near instantaneous access to the data just taken enables the observer to monitor the quality of the system operation and to update the observing procedure based on the preliminary results.

A characteristic of the autocorrelation method of spectral analysis is that the strong galactic hydrogen within the bandpass produces a sinusoidal ripple in the spectrum. This is known as "ringing" and its removal is accomplished by convolving the spectrum with a hanning function. This function is a weighting scheme in which $\frac{1}{2}$ the value of the channel on either side is added to $\frac{1}{2}$ the value of the central channel to produce the new value for that channel. Application of this smoothing worked very well and all data presented here from the 43 m telescope have been smoothed with the hanning function.

A baseline is removed from the data by fitting a low-order polynomial to the spectrum in regions removed from either galactic emission or suspected NGC 185 emission. In practice the order of the fitting polynomial was 2 to 4.

Calibration for this system is done under computer control by periodically firing a noise tube within the receiver and comparing the system output with and without the additional noise. The data are then scaled to this system temperature. The stability of the system was monitored by observing several sources throughout the session. No unexplained drifts in system performance were seen.

CHAPTER III

RESULTS

In this chapter the results of the observations are presented. The carbon monoxide data are treated first, followed by the neutral hydrogen study of NGC 185 and the surrounding region. Only the results are considered in this chapter; the analysis and interpretation of the observations are found in Chapter IV.

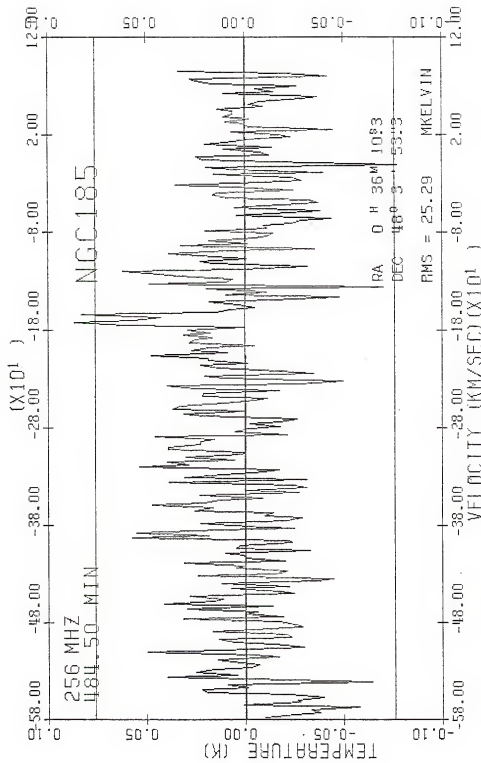
Carbon Monoxide

Positive Result in NGC 185

The dwarf elliptical galaxy NGC 185 was detected at the 115.2712 GHz frequency of ^{12}CO . Figure 2 shows the best spectrum obtained on the source, averaging data from all three observing sessions. The 256 MHz total bandwidth corresponds to about 660 km/sec. The feature is not discernible in the 128 MHz bandwidth spectrum, probably because of the lower signal-to-noise (SN) ratio. Table 1 summarizes the parameters of the spectral feature as measured in Figure 2.

Since the line is only slightly greater than 3 standard deviations, it is very important to be certain of the reality of the feature. One method is to smooth the spectrum with a function (in this case rectangular) of about the same width as the suspected spectral feature. This procedure has the effect of increasing the SN ratio at the expense

Figure 2. The ^{12}CO spectrum for the nucleus of NGC 185. Data from all three observing sessions have been averaged for this spectrum. The total bandwidth for the observation appears in the upper left along with the total integration time on the source. In the lower right the position (1950.0 coordinates) observed is given and the standard deviation for the spectrum is also shown. The baseline at 0.0 Kelvin is shown along with horizontal lines at ± 3 standard deviations.



of velocity resolution. Figure 3 is the result of this convolution, and indeed the reality of the feature is strongly supported.

Table 1
Line Parameters for ^{12}CO in NGC 185

Peak Antenna Temperature (K)	0.081 ± 0.025
Velocity of Line (heliocentric, km/sec)	-175 ± 2
Full-width at Half-maximum (FWHM) (km/sec)	12 ± 2
Position Observed	$0^{\text{h}} 36^{\text{m}} 10^{\text{s}}.3$ $48^{\circ} 3' 53''.3$
Total Integration Time on Source (min)	484.5

Other support for the reality of the line is found by careful examination of the spectra obtained during each session of observing (Figures 4 to 6). The spectral characteristics vary somewhat for each session. But this is to be expected since each individual spectrum has a relatively low SN ratio. In particular the line strengths for each session are

December 1977	$0.20 \pm 0.07 \text{ K}$
July 1978	$0.20 \pm 0.08 \text{ K}$
December 1979	$0.075 \pm 0.028 \text{ K}$

where the quoted errors are 1 standard deviation. In view of the agreement here, and the pointing uncertainty during the December 1979 observations, the discrepancy among the observations is not large.

During the December 1979 observations the cooled receiver operated with two independent channels, linearly polarized and orthogonal to one another. The feature does not appear in the spectrum from the

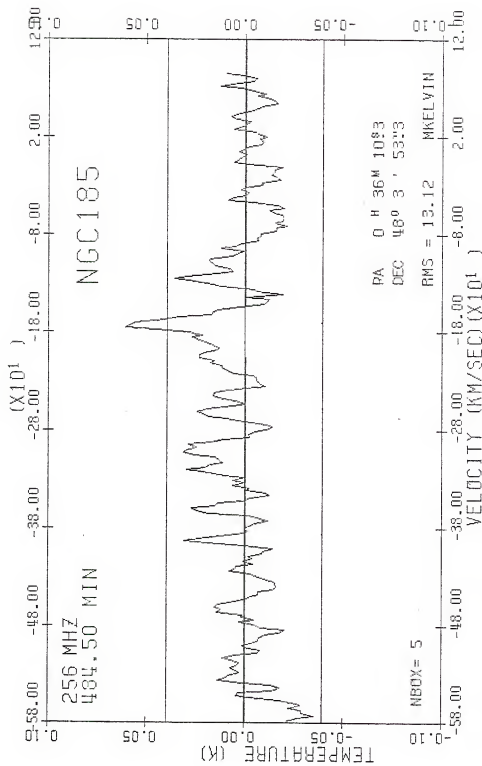
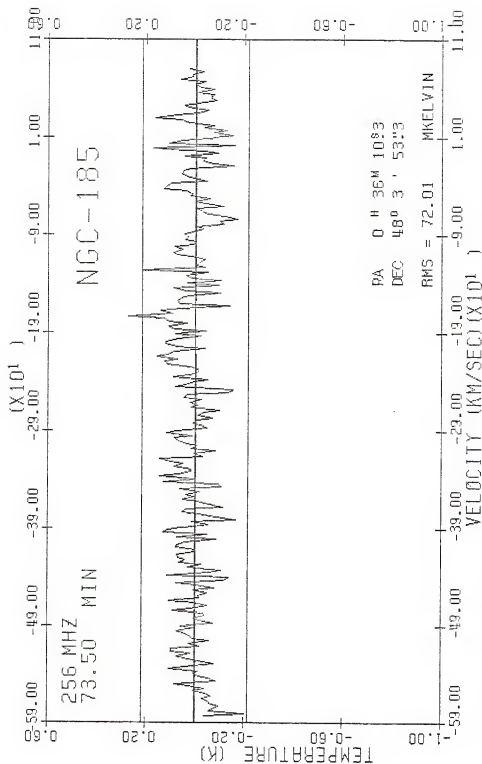
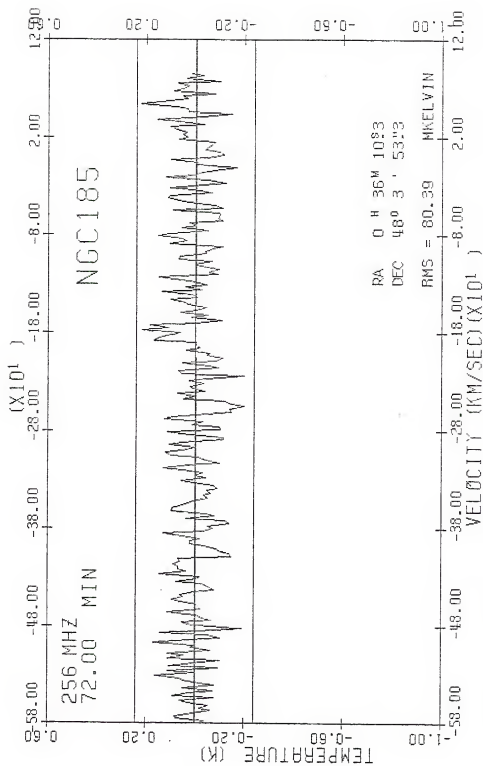


Figure 3. The spectrum of Figure 2 smoothed with a 5 channel (13 km/sec) rectangular function.

Figure 4. The ¹²CO data from December 1977.

Figure 5. The ^{12}CO data from July 1978.

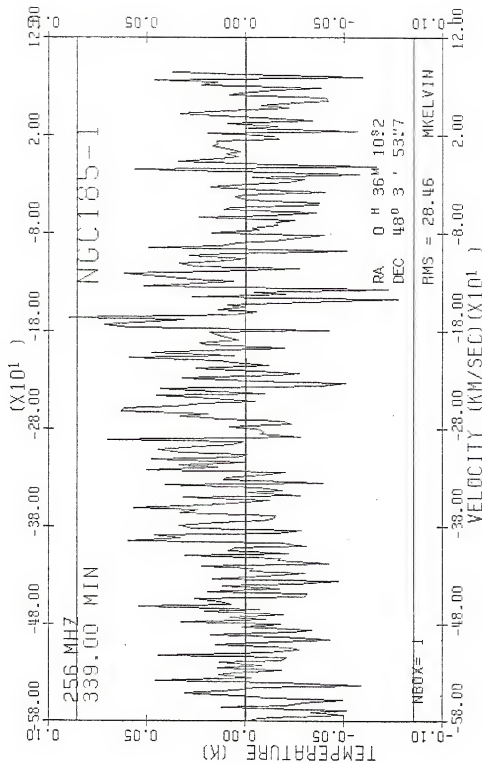


Figure 6. The ^{12}CO data from December 1979, channel A.

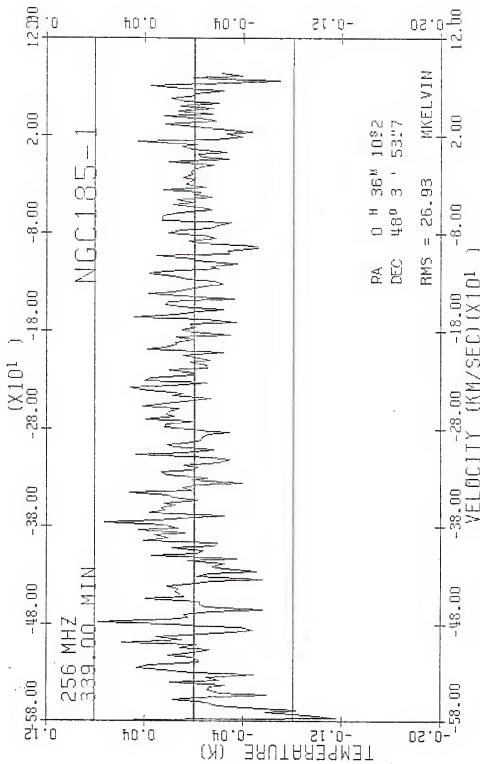


Figure 7. The ¹²CO data from December 1979, channel B.

second channel of the receiver (Figure 7). We have no physical reason to expect a polarized feature and indeed, this transition has never been observed to be polarized in our own galaxy. Also, the tracking procedure rotates the observed polarization planes with respect to the sky; even if the signal were linearly polarized we should be able to detect it in each channel. The lack of a feature in this channel is almost certainly due to the low SN ratio.

A further complication during the December 1979 session was poor pointing corrections for the telescope, especially in regions far from the celestial equator (the declination of NGC 185 is 48°). Consequently we feel that the lack of a feature in the second channel is within the statistical and instrumental uncertainties of the experiment.

Negative Results

A total of 11 early-type systems were observed during the three observing sessions. Our criteria for selecting candidates for CO emission were based on the notion that a system able to retain HI or dust would be more likely to have significant star formation.

Consequently we chose several of the early-type systems that have been detected in HI. Added to the list were galaxies that are close (< 15 Mpc) and also show some form of an ISM. Often this was a notation in the Reference Catalog of Bright Galaxies (RCBG, de Vaucouleurs and de Vaucouleurs 1964) that the system contained obscuring matter.

Table 2 lists the 11 galaxies selected for the CO study. Included are the positions observed, the assumed distance and radial velocities as well as the Holmberg magnitude and the total luminosity. The dates in which useful data were collected are also noted. The final quantity

Table 2
Parameters for Early-Type Galaxies Searched for ^{12}CO

NGC #	$\alpha(1950.0)$	$\delta(1950.0)$	Type	D (Mpc)	V_{\odot} (km/sec)	m_{Holm}	L_{pg} ($10^9 L_{\odot}$)	Dates Observed			1 Standard Deviation (K)
								Dec 1977	July 1978	Dec 1979	
185 (DP-I)	00 ^h 36 ^m 10 ^s .3	48°03'34" E3p	0.69	-245	11.0	0.0267	X	X	X	X	Detected-- see text
185 (DP-II)	00 36 12.2	48 03 27								X	0.025
205-11	00 37 40.7	41 25 33 E5p	0.69	-239	10.1	0.0611		X			0.041
205-12	00 37 41.4	41 24 05								X	0.026
404	01 06 39.1	35 27 08 S0	1.5	-35	11.3	0.0955	X				0.067
1052	02 38 37.0	-8 28 05 E4	11.0	1439	11.1	6.18	X	X	X		0.069
2685	08 51 41.7	58 56 01 S80p	12.0	868	12.0	3.0	X	X	X		0.042
3226	10 20 42.9	20 09 11 E2p	16.5	1356	12.3	4.6	X				0.062
4150	12 08 01.2	30 40 53 S0	3.8	970	12.2	0.267	X	X	X		0.043
4278	12 17 35.7	29 33 33 E1	9.6	659	11.2	4.29	X	X	X		0.057
4636	12 40 17.3	02 57 42 E0	12.5	979	10.4	15.2			X		0.089
5846	15 03 56.5	01 47 50 E0	16.5	2353	11.1	13.9			X		0.140
5866	15 05 07.4	55 57 18 S0	13.8	692	11.0	10.7	X	X	X		0.036

Table 2

Continued

Notes: The positions for NGC 185 and 205 were measured from the Palomar Sky Survey. The positions for the other galaxies are from Galloway and Heidmann (1971), Galloway et al. (1973), or Galloway et al. (1975). The galaxy types and heliocentric velocities are from de Vaucouleurs et al. (1976). The Holmberg magnitude is calculated as described by Galloway et al. (1975).

listed in the table is the standard deviation for all observations of a particular source.

Figures 8-18 show the spectra obtained with the 256 MHz filterbank. Also indicated in the figures are the radial velocity assumed for each source. In many of the spectra there are single channels above or below the 3 standard deviation limit. These are not significant because they fail to persist in further observations. This type of interference is relatively common in multi-channel filterbank receivers, and arises from stray voltages within the equipment. The implications of the negative results are discussed in Chapter IV.

Neutral Hydrogen

The region surrounding NGC 185 was examined to sensitive limits to detect any neutral hydrogen (HI) associated with the galaxy. The 43 m telescope at Green Bank was used in a total power mode as described in Chapter II. The arrangement of "offs" was varied throughout the course of the observing in an effort to delineate the HI detected. One series of observations used an "off" at about 16^m west to allow a reasonable estimate of the total HI content of the region.

Another sequence of observing used closely spaced "offs" (24' or 48') to the west, east, south, and north to get a better idea of the behavior of hydrogen around a specific region. For those observations the "on" was always at the center of the "offs."

Neutral hydrogen was found at significant levels in several regions, both at the position of NGC 185 and several points to the north. Figure 19, which used a distant "off," shows a strong signal of about 14.2 millikelvin (mK) at a radial velocity of -200 km/sec. The

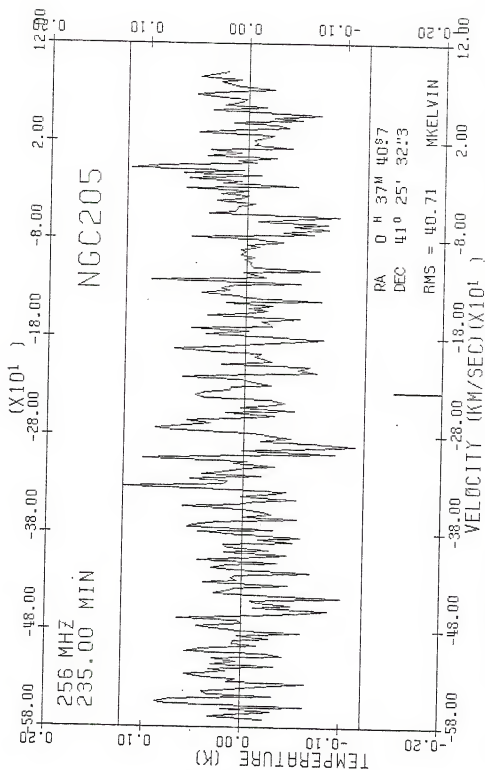


Figure 8. The ^{12}CO data taken in July 1978 on dust patch no. 11 of Hodge (1973) in NGC 185.

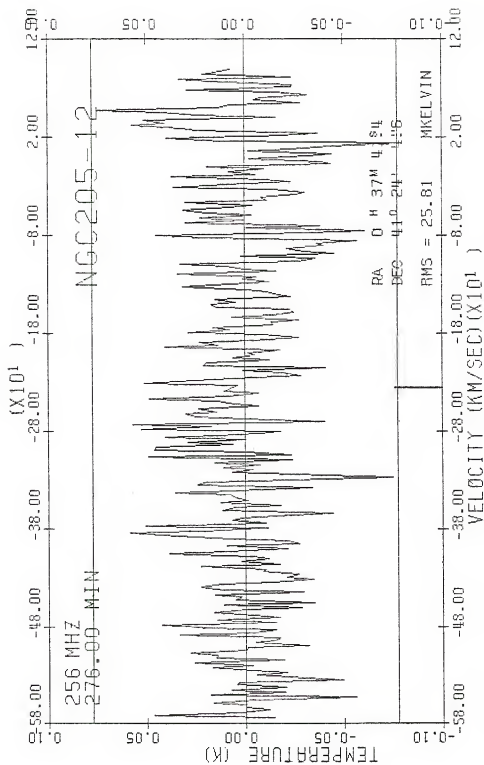


Figure 9. The ¹²CO spectrum obtained in December 1979 on dust patch no. 12 of Hodge (1973) in NGC 205.

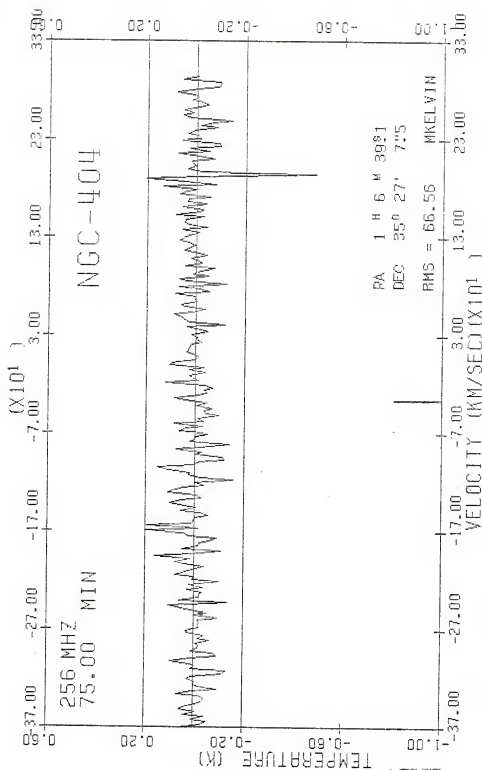


Figure 10. The ^{12}CO spectrum for NGC 404. The negative feature at 200 km/sec is probably not real, but rather an artifact of the multichannel filterbank.

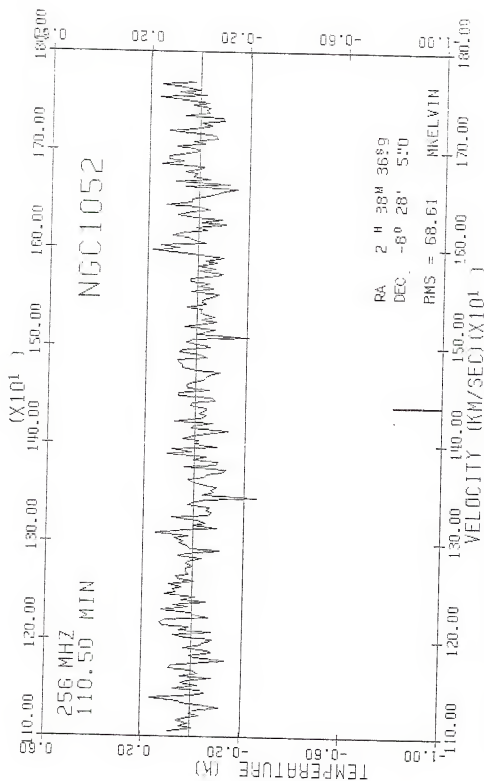
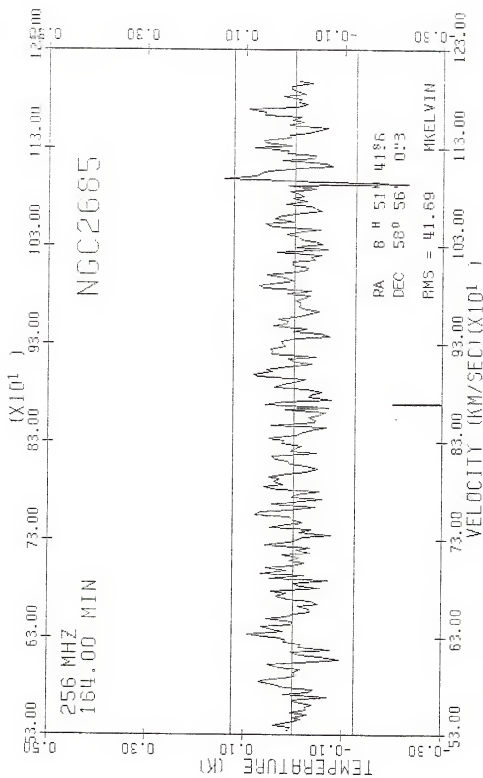
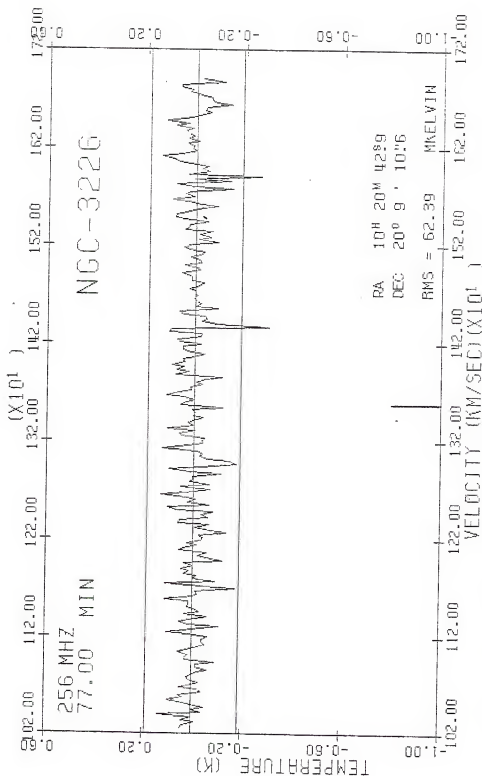


Figure 11. The ¹²CO spectrum for NGC 1052.

Figure 12. The ^{12}CO spectrum for NGC 2685.

Figure 13. The ¹²CO spectrum for NGC 3226.

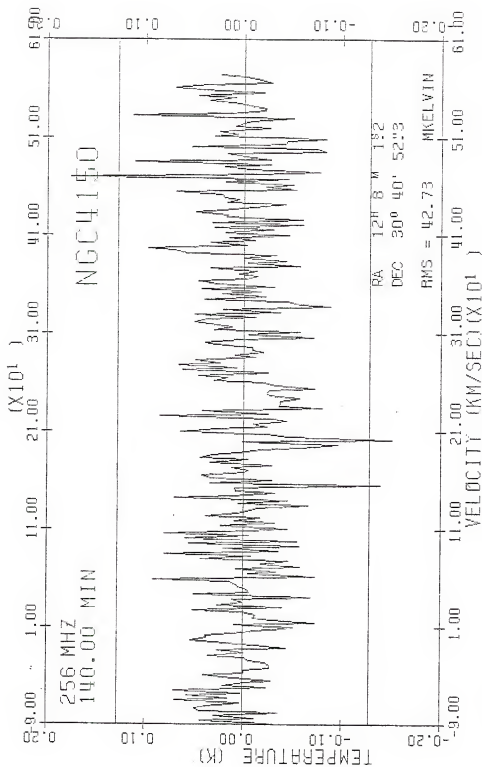
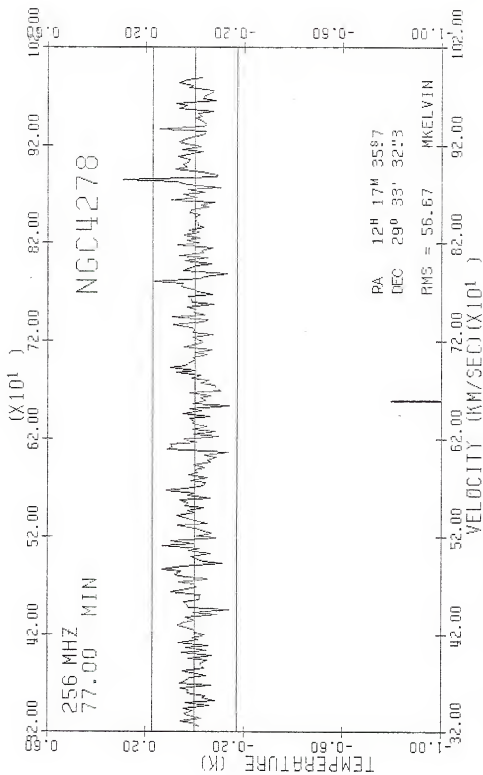


Figure 14. The ^{12}CO spectrum for NGC 4150. De Vaucouleurs and de Vaucouleurs (1964) give a radial velocity of 244 km/sec, but de Vaucouleurs et al. (1976) list it as 970 km/sec.

Figure 15. The ¹²CO spectrum for NGC 4278.

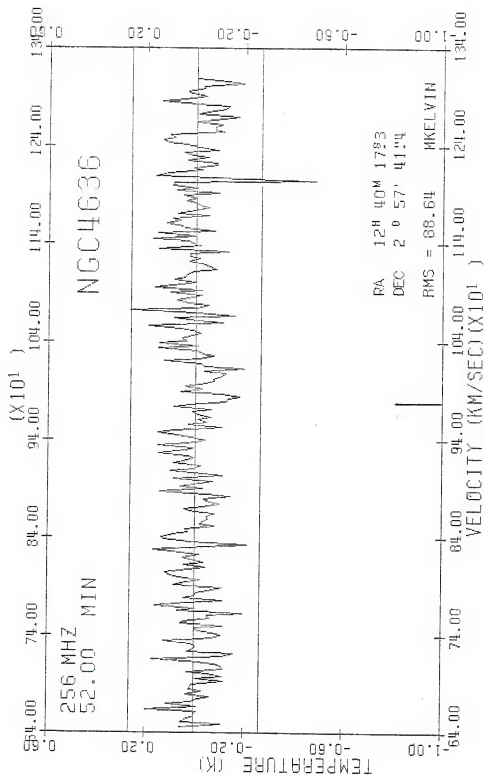


Figure 16. The ¹²CO spectrum for NGC 4636.

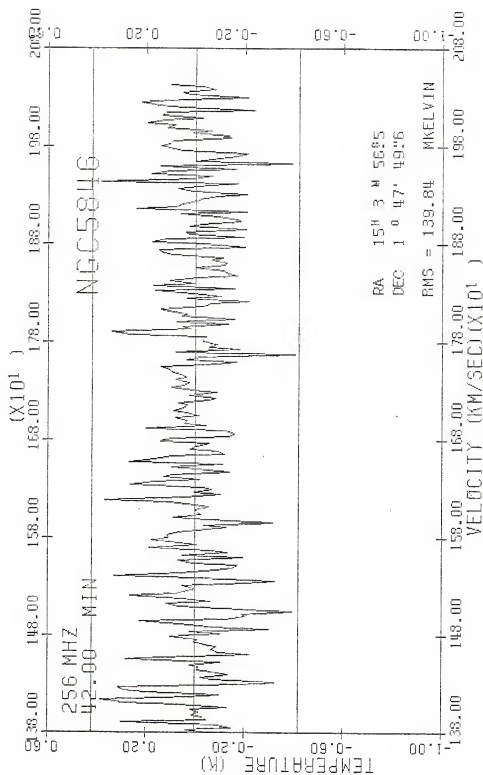
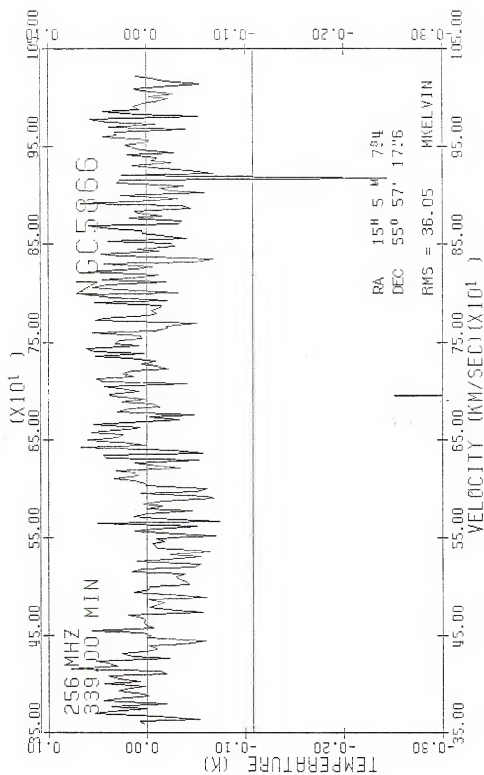


Figure 17. The ^{12}C spectrum for NGC 5846. De Vaucouleurs and de Vaucouleurs (1964) list a radial velocity of 1771 km/sec, but de Vaucouleurs et al. (1976) list it as 2353 km/sec.

Figure 18. The ^{12}CO spectrum for NGC 5866.

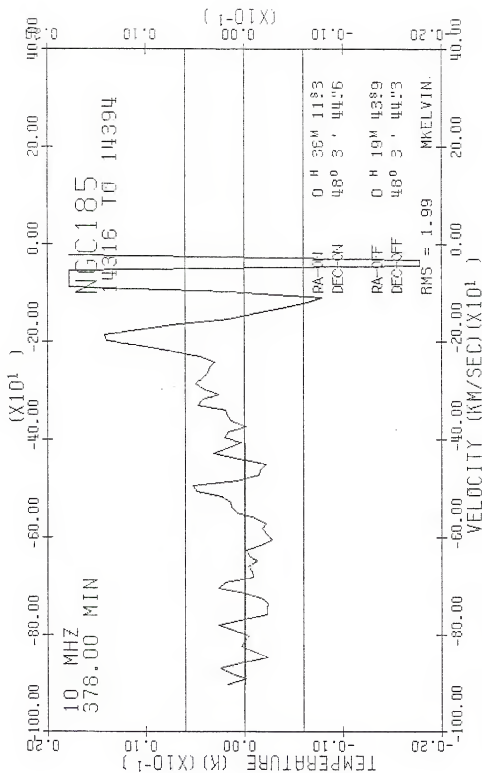


Figure 19. The 21 cm HI spectrum on NGC 185. The off position is indicated in the lower right. The features between -100 and 0 km/sec are local hydrogen.

position of the "on" is at NGC 185. A full-width at half-maximum (FWHM) for the feature is about 60 km/sec.

It is apparent though, from Figure 20, that all of this HI may not be associated with NGC 185. The "offs" for Figure 20 are taken at either 24' or 48' (they have been mixed to increase the SN ratio for this spectrum) in the four cardinal directions. The fact that the signal is only 5.2 mK indicates that some, but not all, of the line has been subtracted out in the "offs."

Further, spectra were generated separately for each of the four directions. Those to the west, east, and south show about a 3 standard deviation positive signal. However, the spectrum with an "off" to the north shows no significant feature in the NGC 185 velocity range.

Continued examination of points to the north of the galaxy reveals a strong 40 mK feature about 70' directly north. The radial velocity of this feature is -180 km/sec with a RWHM of 40 km/sec.

Five point maps of the region to the north also indicate HI signals as far as 2° north and 48' east with a radial velocity of about -180 km/sec. There is only weak HI emission at 49' north of the galaxy. This is shown in Figure 21; the feature is around 15 mK. It appears that there is a ridge or plume of HI that is strongest (43 mK) between 1°-2° directly north of NGC 185. It extends further north and east at a level of around 20 mK.

To the south towards the galaxy the plume decreases in strength to about 10-15 mK. From the sensitive 5-point maps at the position of NGC 185, an excess of about 5 mK is found for the galaxy's location. These observations are summarized in Table 3. The interpretation of these observations is found in Chapter IV.

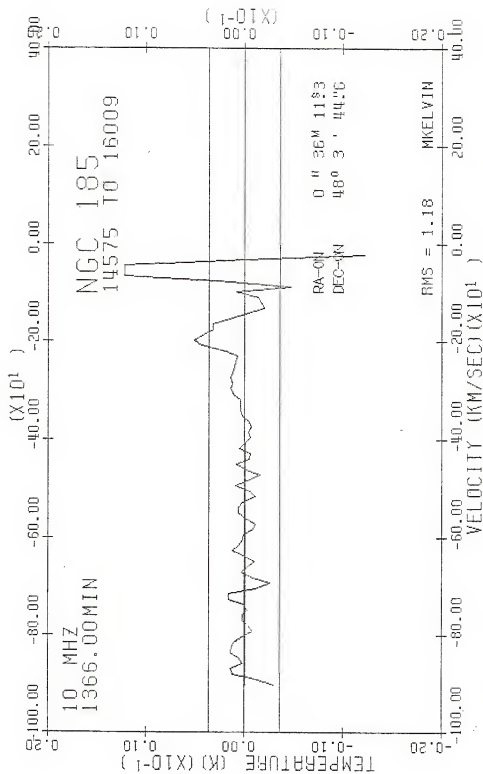


Figure 20. The HI spectrum of NGC 185 with offs 1-2 beam widths to the west, east, south, and north.

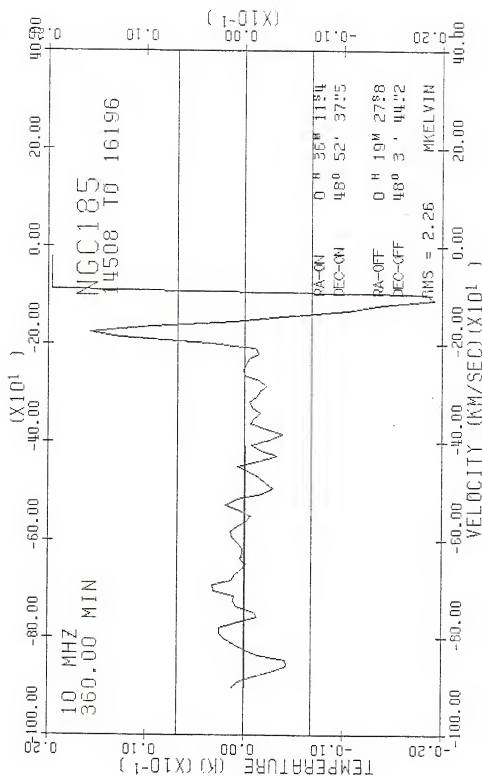


Figure 21. The HI spectrum at 49' north of NGC 185.

Table 3
HI Observations in the Vicinity of NGC 185

Position of ON wrt NGC 185	ON observation		OFF observation		Standard Deviation (mK)	Velocity (km/sec) ± 5 km/sec	Full-width Half-maximum (km/sec) ± 3 K/sec	Time on Source (min)
	$\alpha(1950.0)$	$\delta(1950.0)$	$\alpha(1950.0)$	$\delta(1950.0)$				
NGC 185 ^a	00 36 11.5	48°03'45"	00 19 27.8	48°03'44"	14.4	-190	63	378
49' North ^b	00 36 11.4	48 52 38	00 19 27.8	48 03' 44	15.7	-175	35	360
NGC 185 ^c	00 36 11.4	48 03 44	00 31 19.6	48 03 44	6.1	-200	40	344
NGC 185	00 36 11.4	48 03 44	00 33 45.0	48 03 45	6.3	-200	45	344
			00 41 3.2	48 03 44				
NGC 185	00 36 11.4	47 14 50	00 38 37.7	48 03 44	6.3	-200	45	344
			00 36 11.4	47 14 50				
NGC 185	00 36 11.4	49 14 50	00 36 11.4	47 39 17	<5	--	--	344
			00 36 11.5	48 52 38				
120' North	00 36 11.3	50 03 44	00 36 11.4	48 28 12	-17.3	-200	38	60
			00 41 16.1	50 03 44				
71' North	00 36 11.4	49 14 50	00 36 11.4	49 14 50	-34.6	-180	33	60
			00 19 20	48 03 44				
					39.8	-180	33	13

Notes: These measurements are from spectra reduced using a third order baseline and hanning smoothed. The spectra on NGC 185 with two "off" positions are from data taken at both "off" positions. Approximately 27% of the integration time was with the first "off," the balance with the second "off."

^aReproduced as Figure 19.

^bReproduced as Figure 21.

^cThe sum of this and the three spectra following is reproduced as Figure 20.

CHAPTER IV

DISCUSSION

In this chapter the implications of the observations presented in Chapter III are considered. The simplest calculations from these data involve assumptions about the excitation temperature and optical depth. The portion of the dissertation based on such assumptions is found in this chapter.

NGC 185

This dwarf elliptical galaxy is usually considered to be a companion of M31. It is located about 6° to the north of M31 and the difference in radial velocities is about 55 km/sec. For a discussion of the virial mass of the M31 system and comments on membership in that system see Rood (1979). A distance of 0.69 Mpc is assumed for NGC 185 throughout the following discussion. At this distance $1'' = 1.04 \times 10^{19}$ cm = 3.3 pc.

The classification given by de Vaucouleurs et al. (1976) is E3p. A detailed photographic study of the system by Hodge (1963) shows clearly that the ellipticity (defined by $\epsilon = 1 - \frac{b}{a}$) varies from 0.18 near the nucleus to 0.26 for the outer contours at $350''$ from the nucleus. An increase in ellipticity with radius is commonly observed for elliptical galaxies. The E3 classification (which is based on the outer contours only) is confirmed by Hodge's photometry.

The system is peculiar because of the presence of two dark dust patches within about 20 arcseconds of the nucleus. Figure 22 is an optical photograph of NGC 185 and a schematic of the dust regions is reproduced from Hodge (1963) in Figure 23. Careful comparison of the two figures reveals the extent of the dust in the optical photograph. Table 4 tabulates the positions of the patches used for observation and the areas in square arcseconds and pc^2 as measured from Figure 23. Note that dust patch I (DP-I) has 2 entries, Ia and I. DP-Ia is the dark core of the northwest patch and DP-I is the larger, less dense patch (but also including DP-Ia).

Table 4
Positions, Areas, and Telescope Filling Factors for
Dust Patches in NGC 185

Object	$\alpha(1950.0)$	$\delta(1950.0)$	Area ($"$) ²	pc^2	Filling Factor
DP-Ia	$0^{\text{h}}36^{\text{m}}10^{\text{s}}.3$	$48^{\circ}03'54''$	35	380	0.0072
DP-I	Same as DP-Ia		115	1250	0.0235
DP-II	$0^{\text{h}}36^{\text{m}}12^{\text{s}}.2$	$48^{\circ}03'28''$	350	3800	0.0716
DP-I+II (Center of NGC 185)	$0^{\text{h}}36^{\text{m}}11^{\text{s}}.4$	$48^{\circ}03'44''$	465	5050	0.0951

The CO observations were taken at the position of DP-I in December 1977 and July 1978. The December 1979 observations were made at both DP-I and -II as well as the center of the galaxy. However, as the FWHM for the 11 m telescope indicates in Figure 22, observations of one patch do not entirely exclude the other. Further, the pointing for

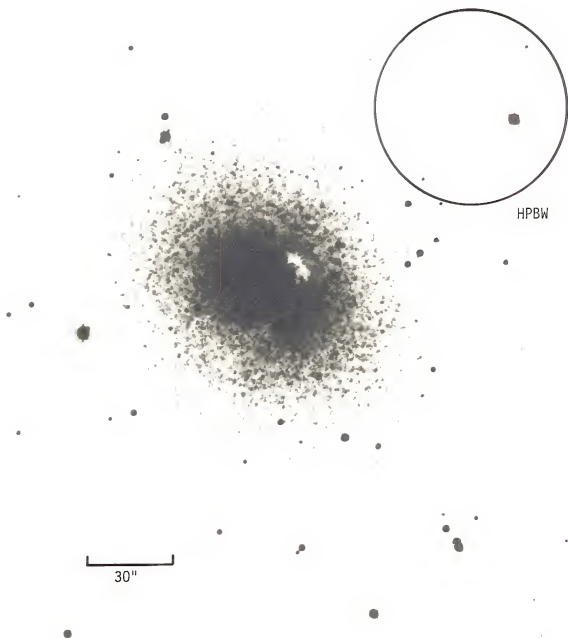


Figure 22. NGC 185 showing the dust patches. North is up and west is to the right. The half-power beam-width is indicated. This photograph is reproduced through the courtesy of Lick Observatory.

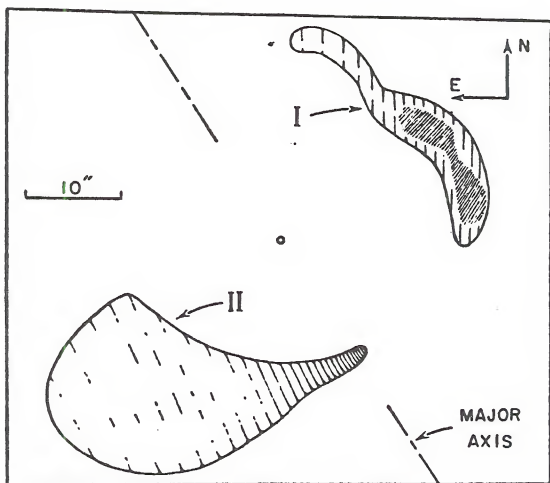


Figure 23. A schematic of the dust regions near the nucleus of NGC 185 (Hodge 1973). DP-I is northwest of the center, DP-II is southeast and DP-Ia is darker region within DP-I.

December 1979 is unreliable to perhaps 20 arcseconds and at times 30-40 arcseconds. Consequently we have no confidence in the apparent identification of the CO source as DP-I based on the absolute pointing.

Because of the uncertainty of the source for the CO emission, the following analysis considers three cases for the calculations of column and particle densities. The individual cases and the assumed CO sources are

Case A	DP-Ia
Case B	DP-I
Case C	DP-I+II

To estimate the kinetic temperature of the molecule we can assume the clouds are optically thick ($\tau \gg 1$). Observations of CO sources within our galaxy indicate that this is often the case with the $J = 1\ 0$ transition (Zuckerman and Palmer 1974). We find (from Appendix II) that

$$T_A^* = \eta_f T_{\text{ex}} \quad (1)$$

where η_f is the forward beam coupling efficiency (also known as the filling factor or the beam dilution) from Ulich and Haas (1976). Since we have no detailed information on the brightness distribution we will assume that $\eta_f = 0.7$ (source area/beam area). The beam area is found from the 65" half-power beamwidth and the factor of 0.7 arises because 30% of the power enters the antenna through the very broad error pattern. Given these assumptions Table 5 gives the expected antenna temperature for the three cases and several excitation temperatures.

Clearly we cannot distinguish between the several possibilities in Table 5 which are consistent with the detected temperature of 0.081 K. But if the CO is optically thick it is unlikely to be above 25 K or to originate in both the clouds.

Table 5
Expected Antenna Temperatures (K) for $\tau \gg 1$

Source	$T_{\text{ex}} = 10 \text{ K}$	25 K	100 K	10^3 K
Case A	0.071 K	0.179	0.714	7.14
Case B	0.235	0.588	2.35	23.5
Case C	0.951	2.38	9.51	95.1

Another approach is to compare the dust clouds observed in NGC 185 to clouds more easily observed in our own galaxy. The disadvantage is that it is not certain that the nature of the clouds will be the same. It does, however, provide a reference point for their study.

The extinction in the dust clouds was measured by Hodge (1963). He finds DP-I to have a mean visual absorption of 0.3 mag but as high as 1 mag in certain parts. The mean for DP-II is measured as 0.15 mag of absorption in the visual.

At this level of absorption the clouds are similar to the diffuse clouds studied by Knapp and Jura (1976). Their study involved clouds situated in front of stellar sources that show color excesses of $E(B - V) \approx 0.3 \text{ mag}$. Assuming a normal $A_V/E(B - V) = 3$ indicates $A_V \sim 1 \text{ mag}$, similar to the absorption in the NGC 185 clouds.

Knapp and Jura suspect optically thin ^{12}CO emission based on their inability to observe ^{13}CO at an intensity of 2-6 times less than the ^{12}CO (usually possible if ^{12}CO is optically thick), and they found antenna temperatures of 1-2 K even though the sources probably filled the beam and had kinetic temperatures of 20 K or more. Using the thin

cloud models of Lucas (1974) and assuming a kinetic temperature of 20 K (Morton 1975) they find that the column density is given by

$$N(\text{CO}) \sim 6.0 \times 10^{14} (T_A^*/n_F) \Delta v \quad (2)$$

where Δv is the full-width half-maximum of the line in km/sec. Using this expression and taking into account beam dilution (n_F) we find column densities for NGC 185 as listed in Table 6.

Table 6
Column density of ^{12}CO for Optically Thin, Diffuse Clouds

Source	$N(\text{CO})$ cm^{-2}	$N(\text{CO}) \times 2 \times 10^4 = N(\text{H}_2)$ cm^{-2}
Case A	8.1×10^{16}	1.6×10^{21}
Case B	2.5×10^{16}	5.0×10^{20}
Case C	6.1×10^{15}	1.2×10^{20}

The mass of the molecular cloud can be found by multiplying the column density of H_2 first by the area of the cloud and then by the mass per particle. The result is $9680 M_\odot$ and is independent of which case is actually correct. It is independent because we are assuming that the source is optically thin and we are detecting all the CO within a given region. Further, it represents a firm lower limit if the colliding particles are H_2 ; if they are HI the minimum mass is $4840 M_\odot$.

The last column of Table 6, total column density of H_2 , is found by assuming $N(\text{CO})/N(\text{H}_2) = 5 \times 10^{-5}$ (Martin and Barrett 1978).

A further finding by Knapp and Jura (1976) is that a necessary, but not sufficient, condition for CO in emission is a particle density $\gtrsim 10^3 \text{ cm}^{-3}$. This agrees with the theoretical result noted in Appendix II. We thus feel confident that the CO emission in NGC 185 is originating in a region at least as dense as 10^3 cm^{-3} .

It would be useful for calculations of the space density of various particles if the physical size of the absorbing regions were known. This would help constrain the various possible sources of the CO emission and help in determinations of the mass of gas involved. An estimate of the cloud volume can be made by assuming they have a dimension along the line-of-sight equal to the average width. This approach will tend to underestimate the volumes unless the clouds are flat and oriented broadside to the line-of-sight. Table 7 tabulates the result of this calculation. The gas mass listed in the last column is found by assuming the entire cloud is filled with molecular hydrogen at a density of 10^3 cm^{-3} .

Table 7
Estimates of Cloud Volumes for NGC 185 Dust Clouds

Dust Cloud	Depth of Cloud (pc)	Volume (cm^3)	Volume (pc^3)	Mass of Gas (M_\odot)
DP-Ia	6.6	7.37×10^{58}	2.5×10^2	6.2×10^4
DP-I	16.5	6.06×10^{59}	2.1×10^4	5.1×10^5
DP-II	42.9	4.79×10^{60}	1.6×10^5	4.0×10^6

Hodge (1963) has estimated the mass of dust in DP-I and DP-II. Using the dust masses and the total gas content for the optically thin

case (Table 6) and the minimum calculated gas mass from Table 7 allows a calculation of the gas-to-dust (G/D) ratio. The results appear in Table 8.

Table 8
Gas-to-Dust Ratios

Cloud	Dust Mass (M_{\odot})	Gas Mass $\tau < 1$ (M_{\odot})	G/D	Gas Mass $\tau \gg 1$ (M_{\odot})	G/D
DP-I	25	9680	390	5.1×10^5	2×10^4
DP-I+II	215	9680	45	4.5×10^6	2×10^4

Considering that the gas-to-dust ratio in our own galaxy is usually quoted as 200, the most attractive source for the CO emission appears to be DP-I.

Using the minimum mass consistent for DP-Ia (Table 6) allows a calculation of the Jeans length for gravitational instability

$$\lambda_J = \left[\frac{\pi k T_K}{4 G \mu p} \right]^{\frac{1}{2}} = 1.6 \left[\frac{T_K^3 R^3}{M_{\odot}} \right]^{\frac{1}{2}} \quad (3)$$

where M_{\odot} is the mass of the cloud in solar masses. Taking the width of the cloud as a characteristic dimension, $R = 6.6$ pc, $T_K = T_{\text{ex}} = 20$ K, and $M = 4.84 \times 10^3 M_{\odot}$

$$\lambda_J = 1.1 \text{ pc}$$

Since the cloud is substantially larger than the Jeans length, it is most likely in a state of collapse.

The Jeans mass can be calculated under these conditions from

$$M_J = \frac{\pi}{6} \rho_0 \lambda_J^3 \sim 10^{23} \frac{(T_K/\mu)^{3/2}}{\rho^{1/2}} \text{ gm} \quad (4)$$

with $T = 20 \text{ K}$, $\mu = 2$, $\rho = 3.34 \times 10^{-21} \text{ g/cm}^3$ (corresponding to 10^3 cm^{-3} of H_2) we find $M_J = 27 M_\odot$. If the cloud remains isothermal as it collapses, and this appears likely because of the effective cooling, M_J decreases and fragmentation is likely to occur.

Another calculation that confirms the collapsing nature of the cloud in NGC 185 is provided by Rowan-Robinson (1979). He estimates the cloud density, in an essentially virial calculation, by the equation

$$n(\text{H}_2) = 10^{3.90} \eta (\Delta v)^2 r^{-2} K_2^{-1} \quad (5)$$

where η is 0.8 for a cloud in equilibrium, r is the radius of the cloud in units of 10^{18} cm , and K_2 is a dimensionless quantity related to a hot core for the cloud (it is always greater than 1.5).

The density calculated for the NGC 185 cloud, assuming 6.6 pc for r (the characteristic width for DP-Ia) is $3.3 \times 10^3 \text{ cm}^{-3}$. If the cloud is in free-fall $\eta = 0.2$ and the derived density is $8.3 \times 10^2 \text{ cm}^{-3}$. Thus considering that the NGC 185 cloud masses are uncomfortably large (Table 7) for higher particle densities, we consider the lower density more likely.

From these arguments it appears that either DP-Ia or DP-I is most likely in a state of collapse. Further, the lack of emission from ionized gas (Humason et al. 1956) implies one of two possibilities. The first is that star-formation ceased in the system long ago, such

that the HII regions associated with massive stars have since dissipated.

Considering that typical lifetimes for HII regions are 10^6 years and Hodge (1973) estimates the age of the OB complex in NGC 205 (very similar to that of NGC 185) to be 5×10^6 years, it is certainly plausible that the early HII regions have evaporated. Since the time for the observed clouds to collapse to stars is about 10^5 years, it seems that the system may be experiencing bursts of star formation similar to that envisioned by van den Bergh (1975).

However, there is a serious flaw in this scenario. Hodge (1963) estimates that the population I stellar component of NGC 185 is about $2 \times 10^5 M_{\odot}$. Using Faber and Gallagher's (1976) mass loss rate of $0.015 M_{\odot} \text{ yr}^{-1} (10^9 L_{\odot})^{-1}$ and the luminosity of NGC 185 ($2.67 \times 10^7 L_{\odot}$), we find that it took 5×10^8 yrs for the material to collect. During the 5×10^6 years since the last star-forming episode only $2 \times 10^3 M_{\odot}$ of gas should have been able to appear. Our CO observations show at least $5 \times 10^3 M_{\odot}$ (for optically thin CO, assuming atomic hydrogen for the colliding particles) and it is likely that there is actually more.

An even stronger case is made if the total mass of dust ($215 M_{\odot}$) is multiplied by an assumed gas-to-dust ratio of 200. The system is seen to contain $4.3 \times 10^4 M_{\odot}$ of gas, more than 10 times the amount from stellar mass loss.

The second possibility that may be occurring in NGC 185 is continual star formation but with no O or B stars, and consequently no HII regions. It is very difficult to prove that this is the process taking place. If indeed low-mass stars are being formed they will be too faint to see and deductive reasoning is necessary to support this

possibility. Specifically, since the regions observed are dense enough to form stars yet no HII regions are observed, either no stars have formed yet (leading to the burst hypothesis) or only low-mass stars are forming.

The idea of a skewed mass distribution for stars is explored in some details by Mezger and Smith (1977). They find that clusters of massive stars (which produce giant HII regions) are found only along spiral arms. It is probable that the spiral shock front of a density wave triggers their formation. It appears though, that the low-mass stars can form out of small but dense clouds (Herbig 1970) that are far more widespread than large clouds.

Jura (1977) also proposes that the expected radiation environment of elliptical galaxies (low UV flux) will lead to low-mass star formation. The reasoning is that the low flux results in less heating of the clouds. A cooler cloud will have a lower critical mass which can separate out and collapse to form a star.

The dynamics of the nuclear region will be considered in the following paragraphs. The difficulties in measuring radial velocities for early-type galaxies are immense. There are usually no HII regions in these galaxies so their sharp emission lines are not available for measurement. The absorption lines from the stars are intrinsically wide and further broadened by the stellar velocity dispersion, resulting in large errors.

The radial velocity data for NGC 185 are actually better than that for most early-type galaxies. Ford et al. (1973) identified four planetary nebulae in the system and later Ford et al. (1977) succeeded in measuring the radial velocities of two of these objects, NGC 185-1 and

-2 in their notation. These measurements, coupled with the radial velocity of DP-I, can be used to calculate a rough mass interior to the object and, when combined with the isophotal contours of Hodge (1963), the mass-to-luminosity ratio (MLR) can be computed.

Table 9
Positions and Radial Velocities of Points Within NGC 185

Object	Radial Velocity (km/sec)	Distance from Minor Axis (pc)	Distance from Major Axis (pc)
185-1	-212.5	144.2	75.6
185-2	-200	107.3	103.6
DP-I	-175	0	43.9

Table 9 lists the three radial velocities determined for the system, as well as the projected distances from the major and minor axes. We make the simple assumption that the ellipticity is caused by rotation about the minor axis, thus the figure of the system is an oblate spheroid. We further assume that the radial velocities are the projected results of purely circular velocities about the nucleus. We can then make a straightforward calculation of the mass interior to the measured point. Implicit in this approach is the assumption that the points lie in the plane of the galaxy.

Recalling the work of de Vaucouleurs (1977), described in Chapter I, on the relative frequencies of various ellipticities, we can make an informed guess of the true ellipticity of NGC 185. The galaxy is most likely to be an E3.6, but we can be more flexible and also consider

the possibility that it is an E5.5 (the flattest elliptical according to de Vaucouleurs 1977). Of course the system may be an E3 seen face-on, but the velocity gradient for the three measured points strongly suggests rotation.

The details of the determination of the inclination angle (i , defined to be the angle between the plane of the galaxy and the plane of the sky) and its effects on other parameters are found in Appendix III. Under the assumption that the system as is an E3.6 or an E5.5 the inclination angle is 53.1° or 68.0° , respectively.

The azimuthal angle, θ' , can be deprojected to find the true azimuthal angle, θ . The results are contained in Table 10 for the two planetary nebulae. Since DP-I lies on the minor axis we assume it has no radial velocity due to rotation; consequently we take its radial velocity, -175 km/sec, as the systemic velocity for the galaxy.

Table 10
Values for the Observed and True Azimuthal Angles

Object	θ' (degrees)	θ (degrees)	
		$i = 53.1^\circ$	$i = 68.0^\circ$
185-1	26.8	40.1	53.4
185-2	44.0	58.1	68.8

The true circular velocity for the nebulae can thus be calculated from

$$v_c = v_r / \cos \theta \sin i \quad (6)$$

The true radius can also be computed and is listed with the velocities in Table 11. Finally, the mass interior to the point, assuming Keplerian motion, is given by

$$M = 2.36 \times 10^2 v_c^2 r \quad (7)$$

where M is in solar masses, v is the circular velocity in km/sec, and r is the true radius in parsecs.

Table 11
Circular Velocities and Radial Distances in NGC 185

Object	v_r km/sec	v_c (km/sec)		r (pc)	
		$i = 53.1^\circ$	$i = 68.0^\circ$	$i = 53.1^\circ$	$i = 68.0^\circ$
185-1	37.5	61.3	67.8	191.4	248.0
185-2	25	59.2	74.6	203.2	296.6

The isophotal contours of Hodge (1963) were measured to find the luminosity interior to a given point. The contours measured were the innermost (1) and the next brightest (2), corresponding to 20.47 and 21.22 mag/arcsec², respectively. Using a distance modulus of 23.9 and assuming absorption within our own galaxy according to the cosecant law ($A_V = 0.26 \csc b = 1.0$ mag for NGC 185) allows the calculation of the luminosity interior to the first and second contours, listed in Table 12.

Table 12
Luminosities in the Nucleus of NGC 185

Contour	Brightness ₂ (mag/arcsec ²)	Area (arcsec ²)	Luminosity (L _☉)
1	20.47	1690	1.03×10^7
2	21.22	7715 ^a	2.35×10^{7a}

^aExcludes contribution interior to contour 1.

The mass calculated from equation 7 is then divided by the appropriate luminosity from Table 12 to derive the MLR interior to each object. The Planetary nebulae, 185-1, lies on the second contour, making the luminosity interior to it the sum of the luminosities inside contours 1 and 2. The other nebula, 185-2, lies midway between contours 1 and 2 so we use the luminosity inside 1 plus half the luminosity inside 2. Table 13 lists the results for the MLR derived with these values.

Table 13
Mass-to-Luminosity Ratios for the Nucleus of NGC 185

Object	Mass Interior (M _☉)		Luminosity (L _☉)	MLR (solar units)	
	i = 53.1°	i = 68.0°		i = 53.1°	i = 68.0°
185-1	1.7×10^8	2.7×10^8	3.38×10^7	5.0	8.0
185-2	1.7×10^8	3.9×10^8	2.21×10^7	7.7	17.6

While these values for the MLR are very reasonable for early-type galaxies in general (Faber and Gallagher 1979), there is a significant disagreement with the MLR of 1.8 used by Ford et al. (1977) for NGC 185 and NGC 147. This MLR is ostensibly derived from observations of M32. We feel that the most likely cause for the discrepancy is that Ford et al. (1977) do not consider possible rotation in their analysis. The radial velocity of DP-I is most likely nearest the systemic velocity of NGC 185 since it is fortuitously on the minor axis.

We find that the MLR of the nuclear regions of NGC 185 is between 5 and 18. Considering the non-linear effects of the inclination and azimuthal angle, the most likely value for the MLR is around 8. Assuming that it is independent of radius, the total mass of NGC 185 is found to be $1.3 \times 10^9 M_{\odot}$.

NGC 205

Another dwarf elliptical companion of M31, NGC 105, was also observed to sensitive limits for CO emission, with negative results. Figures 8 and 9 show the averaged spectra from the July 1978 and December 1979 sessions, respectively. The spectra are taken at two different positions within the galaxy (dust patches 11 and 12 in Hodge's (1973) notation). Hodge (1973) describes and diagrams the dust content of NGC 205. The distribution is reminiscent of NGC 185 but with a larger number of discrete clouds over a wider region in the nucleus. The July 1978 observations

were taken on dust patch number 11 while the December 1979 observations were of dust patch number 12 on the other side of the nucleus. Table 14 lists the positions observed for each patch as well as Hodge's (1973) estimates of the dust content. The dimensions listed by Hodge are used to find a rough area in square arcseconds and pc^2 (the assumed distance is 0.69 Mpc). Hodge (1973) also presents microphotometer tracings of these dust regions indicating a visual absorption of about 0.2-0.3 magnitudes. It is clear that these regions are not as dense as DP-Ia in NGC 185. Beyond this difference the two galaxies are very similar in dust and young star content.

Table 14
Dust Regions in NGC 205

Region no.	$\alpha(1950.0)$	$\delta(1950.0)$	Area of (") ²	Cloud pc^2	Dust Mass M_{\odot}
11	0 ^h 37 ^m 40 ^s .7	41°25'33"	360	3.9×10^3	160
12	0 37 41.3	41 24 05	880	9.6×10^3	460

A similar calculation as was made for the NGC 185 dust clouds, under the assumption of optically thin emission (see equation (2) of this chapter), can be performed. The antenna temperature used is 3 times the standard deviation for each cloud. The velocity width is taken to be four times the channel width ($\Delta v = 10.4$ km/sec). The results appear in Table 15. The column densities are modest when compared to those of NGC 185 (Table 6). The computed total masses are even less than one may expect from the dust masses and a gas-to-dust ratio of 200,

3.2×10^4 and $9.2 \times 10^4 M_{\odot}$ for clouds 11 and 12, respectively.

Table 15
Maximum Column Densities of CO and H₂ for NGC 205, $\tau < 1$

Cloud no.	N(CO) (cm ⁻²)	N(H ₂) (cm ⁻²)	M (molecular) M_{\odot}
11	7.0×10^{15}	1.4×10^{20}	4.4×10^3
12	2.8×10^{15}	5.6×10^{19}	5.2×10^3

The situation does not change if one assumes the clouds are optically thick. The NGC 205 clouds are relatively large compared to those in NGC 185, and any reasonable kinetic temperature will produce a large antenna temperature, as shown in Table 5, very easily.

The question is then, why is NGC 205 not detected while NGC 185 with similar morphology (and actually less dust) is detected at the frequency of ¹²CO?

We feel that the key difference in the two systems is that the NGC 205 clouds are less dense than those in NGC 185. Hodge's (1963 and 1973) microphotometer tracings show this, and even optical photographs of the two galaxies show the NGC 185 dust patches to be more prominent.

As Knapp and Jura (1976) found, even a density of 10^3 cm^{-3} is not sufficient to ensure detection of ¹²CO in emission. Further, their observations were made on nearby clouds where one could reasonably expect a filled beam. The NGC 205 observations involve substantial beam dilution which considerably worsens prospects for detection.

While many of the arguments about continuing star formation in NGC 205 can be advanced with much the same reasoning as those for NGC 185 in the previous section, much of this support is lost because we cannot be sure the NGC 205 clouds are in a state of collapse. However, it is very likely that they will eventually form stars. This is clear because NGC 205 has an even larger young stellar component than NGC 185; Hodge (1973) calculates some $2 \times 10^6 M_{\odot}$ for the young stars.

We seem to be seeing an earlier stage of the process in an elliptical galaxy which converts the ISM into stars. In a few times 10^5 years the dust clouds in NGC 205 will be much more condensed and CO emission should be detectable. In the future stars will be forming and, if these are high-mass stars, the galaxy will retain its unusual population I component.

Negative CO Results

The galaxies that were not detected at the $^{12}\text{CO } J = 1 \rightarrow 0$ transition are listed in Table 2. Several attributes are also listed, along with the limits of our observations. These limits can be interpreted on the basis of two assumptions about the CO.

First is that the gas is optically thin and the emission was not detected because of beam dilution or an exceedingly small optical depth ($\tau \ll 1$). Second, if the line is optically thick then beam dilution is the only mechanism to lower the antenna temperature below our detection limits.

Another variable in the interpretation of these negative results is the width of the undetected CO line. If it is several hundred km/sec broad, representing the contributions of many small clouds within the

beam, it is more difficult to detect than if it were a narrow feature arising from only a single, larger cloud.

If $\tau \gg 1$ no information can be gained about the amount of molecular material stored. Essentially any quantity of material can be stored in clumped, optically thick clouds. The material remains undetected because of the very small filling factor (η_f). Consequently Table 16 lists various parameters under the assumption that the CO clouds are optically thin.

Knapp and Jura's (1976) finding that the ^{12}CO line is probably thin if the visual absorption is less than 1 magnitude indicates that most CO in elliptical galaxies will be thin since deep absorption features are rare.

Equation (2) from this chapter is used along with the assumption of $\eta_f = 0.05$. The antenna temperature is taken to be 3 times the standard deviation listed in Table 2. The width of the undetected feature is taken to be 10 km/sec for one set of calculations and 200 km/sec for a second set. The first width is appropriate for a single cloud while the second is more typical of an expected global profile for many clouds (Rickard et al. 1977).

Also listed is the column density of H_2 assuming $N(\text{CO})/N(\text{H}_2) = 5 \times 10^{-5}$ (Martin and Barrett 1978). The molecular mass is calculated by (Schneps et al. 1978)

$$M = \Omega(T_{\text{ex}})(T_A^*/\eta_f)\Delta v D^2 \quad (8)$$

where M is the molecular mass in solar masses, $\Omega(T_{\text{ex}})$ incorporates the effect of temperature on the population levels of the CO, T_A^* is taken to be 3 times the standard deviation, Δv is the assumed velocity width

Table 16
Maximum Molecular Masses Derived from CO Observations

NGC #	3x rms (K)	$\tau < 1, \Delta V = 10 \text{ km/sec}$			$\tau < 1, \Delta V = 200 \text{ km/sec}$		
		N(CO) (10^{16} cm^{-2})	N(H ₂) (10^{20} cm^{-2})	Mass T=20 K (M_{\odot})	N(CO) (10^{16} cm^{-2})	N(H ₂) (10^{20} cm^{-2})	Mass T=20 K (M_{\odot})
205-11	0.123	1.48	3.0	1.2×10^4	29.6	59.2	2.4×10^5
205-12	0.078	0.936	1.9	7.4×10^3	18.7	37.4	1.5×10^5
404	0.201	2.41	4.8	9.0×10^4	48.2	96.2	1.8×10^6
1052	0.207	2.48	5.0	5.0×10^6	49.6	99.2	1.0×10^8
2585	0.126	1.51	3.0	3.6×10^6	30.2	60.4	7.2×10^7
3226	0.186	2.23	4.5	1.0×10^7	44.6	89.2	2.0×10^8
4150	0.129	1.55	3.1	3.7×10^5	31.0	62.0	7.4×10^6
4278	0.171	2.05	4.1	3.2×10^6	41.0	82.0	6.4×10^7
4636	0.267	3.20	6.4	8.3×10^6	64.0	128	1.7×10^8
5846	0.420	5.04	10.1	2.3×10^7	101	202	4.6×10^8
5866	0.108	1.30	2.6	4.1×10^6	26.0	52.0	8.2×10^7

^aUnwin (1980)

^cGallagher et al. (1978)

^eBottinelli and Gouguenheim
(1977b)

^bReif et al. (1978)

^dKnapp et al. (1978c)

^fHuchtmeier et al. (1977)

^eBottinelli and Gouguenheim
(1977b)

^fHuchtmeier et al. (1977)

in km/sec, and D is the distance to the source in Kpc. For $T_{\text{ex}} < 3000$ K the vibrational levels of CO are not populated and $\Omega(T_{\text{ex}}) \sim 10^{-3} T_{\text{ex}}$.

Also listed in Table 16 is the mass of HI that has been detected in the galaxy. The last column gives the expected HI content from Knapp et al. (1978c)

$$M_{\text{HI}} = 4.4 \times 10^7 (L_{\text{pg}}/10^9 L_{\odot}) \quad (9)$$

where M_{HI} is in solar masses and L_{pg} is the photographic luminosity of the galaxy. This relation uses the mass loss rate given by Faber and Gallagher (1976) of $0.015 \text{ yr}^{-1} (10^9 L_{\odot})^{-1}$ and assumes a time for accumulation of 4×10^9 yrs, the time over which we are sure that normal elliptical galaxies have existed (Gunn and Oke 1975). A decrease of 25% is made to allow for an undetectable helium contribution.

Caution must be exercised in comparing the expected HI content with the maximum molecular content as derived here. First they are correct only if the CO is optically thin. While there is reason to believe this is the case, it is not certain. For an optically thick cloud only the surface is seen and no information is available about the total mass.

Second, the CO observations are made with a 65" HPBW while the galaxies are typically several times this size. The CO-implied estimates of the total gas are thus only true for the central regions, whereas the expected HI is for the entire galaxy. Indeed, in the cases of the detected HI the beam is usually about the size of the galaxy.

This discrepancy in the size of the regions sampled may not be an important consideration. This is due to the difficulty of finding

a mechanism that would allow the gas to maintain the same spatial distribution as the stars that shed it. As long as the gas can cool itself effectively, usually via line radiation, it must collapse into the potential well of the galaxy. If it cannot cool itself, a galactic wind sets up and the system is swept clean. The point has been made previously that galactic winds are not universally effective, consequently one expects the interstellar material to preferentially collect in the nucleus.

Comparing the maximum reasonable amount of molecular material that could escape detection under these assumptions ($\tau < 1$, $\Delta v = 200$ km/sec) with the expected HI content reveals that molecular storage is not a dominating feature of the galaxy's ISM. The largest discrepancy, for NGC 205, may not be significant because the region sampled for CO is small with respect to the dust patches.

For the other galaxies the discrepancy may be due to one, or a combination, of three processes: the gas may be clumped and thus optically thick, the material could have been removed either by a galactic wind or ram-jet stripping, or finally, star formation could be consuming the gas with an IMF deficient in high-mass, bright stars.

A fourth possibility, that the clouds are similar to Knapp and Jura's (1976) thin clouds with $n \sim 10^3 \text{ cm}^{-3}$ but with no CO emission, is unlikely. The CO observations included a large portion of the galaxy's nucleus and it seems highly improbable that all the clouds will be in this nether region of collapse with no CO emission. Certainly some fraction may be without CO emission but others, further collapsed, should produce CO emission.

It is interesting to note that the three galaxies with a detected HI content larger than expected (NGC 1052, 2685, and 4278) are all suspected of accretion. All three systems show peculiar dynamics for the HI that make an extra-galactic source the most plausible explanation (Reif et al. 1978, Shane 1980, Knapp et al. 1978c).

Neutral Hydrogen and NGC 185

As described in Chapter III, we have detected neutral hydrogen at the position of NGC 185. There is also detectable HI at least as far as 2° north of the galaxy. It is apparent that any HI physically associated with NGC 185 is being confused with high-velocity hydrogen belonging to our own galaxy.

The mass of HI in a particular feature is given by (Wright 1974)

$$M_{\text{HI}} = 2.356 \times 10^5 D^2 \int S \, dV \quad (10)$$

where the mass is in solar masses, D is in Mpc, S is the flux density in Janskys (1 Jansky = $10^{-26} \text{ W m}^{-2} \text{ Hz}^{-1}$), and dV is in km/sec. This equation is based on the assumption of low optical depth in the 21 cm line. While this assumption may not be valid in the plane of the galaxy, it is quite likely true for HI out of the plane (NGC 185 is at a galactic latitude of -15°).

The confusion with high-velocity local HI is primarily due to the Magellanic Stream, an arc of HI clouds stretching from the Magellanic clouds through the south galactic pole and terminating in the vicinity of NGC 185 (Mathewson et al. 1974).

That there are indeed discrete clouds in the velocity range around -200 km/sec and within 4°-6° of NGC 185 is confirmed by Giovanelli (1979) and Hulsbosch (1980). Hulsbosch's observations of the area show nothing at either the position of the galaxy or within 2° to the north. This lack of confirmation of our findings is not surprising because Hulsbosch's sensitivity is only about 400 mJy while ours is about 25 to 40 mJy (the 43 m telescope has a sensitivity of about 4 Jy/K).

Based on our observations it is clear that there is HI around NGC 185 with a distribution greater than $24'$. Figure 19 shows a feature with about 15 mK of HI when the "off" is located many beamwidths to the west. When a spectrum is taken with the "offs" only $24'$ or $48'$ to the west, east, south, and north, the strength of the feature drops to around 5 mK. This clearly indicates that we are subtracting out about 10 mK of broadly distributed HI.

Analysis of the individual spectra with an "off" in one of the four cardinal directions shows that there is an excess of HI with respect to all directions except perhaps the north. The intriguing possibility is that while there is clearly a broadly distributed HI components around NGC 185, the spectra show that there is excess line radiation from the position of the galaxy when compared with areas 1 to 2 beamwidths away.

Of course it is possible that an enhancement in the high-velocity cloud coincidentally projects onto NGC 185. Our observations are not sensitive enough nor spatially resolved enough to answer the question definitively.

It is interesting to note that if the 5 mK excess does originate in NGC 185, the mass associated with it is about $9 \times 10^4 M_{\odot}$. This is quite reasonable since the minimum molecular mass needed to generate the observed CO signal is $10^4 M_{\odot}$. Indeed, a calculation of the mass of HI expected in the galaxy from normal stellar evolution (see equation 7, in the previous section) is $1.2 \times 10^6 M_{\odot}$.

A final possibility suggested by the detection of a plume between 1° and 2° further north of the galaxy is that we are seeing a tail or streamer of HI associated with NGC 185. Since the galaxy is a

companion of M31 an interaction of this sort may be occurring. The difficulty is that M31 is to the south of NGC 185 and is over 6° away, a rather larger distance for an interaction considering the small mass of NGC 185. Thus while the intergalactic plume is an intriguing possibility, it is not well-supported by our observations.

Higher spatial resolution measurements are required in the area centered on the galaxy and at least 20-30' around. It is necessary to examine the local features well enough to allow their subtraction from possible HI belonging to NGC 185.

Any HI associated with the galaxy would probably have a distribution less than 5' across; the galaxy itself has a major diameter of around 10'. The VLA can easily achieve this resolution, and an investigation of the NGC 185 region should be undertaken to determine the kinematics of the HI at the position of the galaxy.

CHAPTER V

SUMMARY

The current understanding of elliptical galaxy formation and evolution has several important shortcomings. It is not understood how elliptical, or for that matter any, galaxies separate out from the background and collapse. Even the general process of whether the clusters of galaxies form before the individual galaxies is not clear.

The deceptively relaxed-looking stellar distributions are apparently not relaxed at all. It is quite possible that the 3-dimensional figure of elliptical galaxies is actually a triaxial ellipsoid. Further inconsistencies are apparent in the disposition of gas shed by the stars within the galaxy. If it recycled into stars with a normal IMF the nuclei of all early-type systems should be bluer than observed.

Recent theoretical work has shown that two gas removal mechanisms may be present in these systems. One is a galactic wind in which supernovae provide an energy source to heat the ISM of the galaxy to a temperature high enough to evaporate from the system. The crucial points of this method are the assumed Type I supernova rate and the efficiency of energy coupling between the expanding supernova shells and the general ISM.

The other mechanism is ram-jet stripping. The process is basically a hydrodynamic interaction between an assumed intracluster medium and the ISM of the galaxy. There is circumstantial evidence for this

process; early-type galaxies are preferentially found in rich clusters that would be most effective in retaining an intracluster medium. However, it is not clear that the presence of early-type systems in rich clusters is not a result of initial conditions at the time of the cluster formation. Indeed recent work has tended to support this view.

Observations of nearby galaxies do not fit well with either of the two mechanisms. Some have been detected in HI when the galaxy should be able to expel its ISM. Worse, in at least two cases the HI has a broad distribution, entirely contrary to expectations for a partially operating galactic wind or ram-jet stripping. The suggestion has been made that the HI has recently been accreted, but this is difficult to support based on the space density of HI clouds large enough to account for the material. Other early-type galaxies show patches of obscuring matter firmly indicating that mass removal processes are not completely efficient.

Observations of ^{12}CO were undertaken for early-type galaxies to determine the role of star formation in the removal of the ISM. The CO molecule was chosen because it is widely distributed, resistant to dissociation, and has a transition frequency accessible to highly sensitive radio telescopes.

The $J = 1 \rightarrow 0$ transition of ^{12}CO was detected in the dwarf elliptical galaxy NGC 185. The physics of the line formation process strongly imply that the emitting region is the north-west dust patch about 15 arcseconds from the nucleus. The fact that the line is seen at all indicates that the region is at least as dense as 10^3 cm^{-3} . The minimum mass consistent with the observations is about $10^4 M_{\odot}$.

A region as large as this dust patch is gravitationally unstable and is collapsing, probably forming stars at a later epoch. The nucleus of NGC 185 contains several bright blue, presumably young stars which have formed in the relatively recent past.

Observations of another dwarf elliptical galaxy, NGC 205, failed to find CO emission even though this galaxy contains a larger population of young stars and more total dust content distributed in 12 patches. The densest of the regions are not as dense as the northwest dust patch of NGC 185. It is suggested that this is the primary reason for not detecting NGC 205 while obtaining a positive result on NGC 185.

Negative results for 9 other early-type systems are presented and the implications are discussed. The major finding is that the material shed by the stars cannot be contained in optically thin clouds and still elude detection in these observations. Alternatives are that the gas is clumpy and thus optically thick, it has been swept out by either a galactic wind or ram-jet stripping, or it is being consumed by star formation with an IMF skewed towards low-mass stars.

Theoretical support for a skewed IMF is presented, but the question cannot be answered by observations with present-day equipment. More sensitive CO data are needed and the interaction between the intra-cluster medium and the ISM needs to be explored further.

Using radial velocities from two planetary nebulae in the system we find convincing evidence that the galaxy is rotating about its minor axis. The data can be further used to derive the mass interior to the measured points. Of course some basic assumptions about the true ellipticity of the galaxy and the effect of projection onto the plane

of the sky preclude firm conclusions about the dynamics of the system.

We find, however, that the mass-to-luminosity ratio in the nucleus (the planetary nebulae are both within 1 arcminute of the nucleus) is between 5 and 18, with the most likely value around 8. This number is quite reasonable for an early-type system, but the difficulty in determining the ratio, and the lack of agreement from different methods, prohibit any conclusions beyond those already mentioned.

Neutral hydrogen observations of the vicinity of NGC 185 are presented. They reveal the probable existence of high-velocity hydrogen at -180 km/sec at and near NGC 185. The observations also show an enhancement of about 5 mK antenna temperature at the position of the galaxy with respect to 1-2 beamwidths away. The data are inadequate to determine if the material is in NGC 185 or is just an enhancement in the local material coincidentally superposed on NGC 185.

APPENDIX I
CALIBRATION THEORY FOR CO OBSERVATIONS

The intent of the calibration procedure is to correct the data for several factors that distinguish a real telescope at the earth's surface from an ideal telescope at the top of the atmosphere. The major correction factors are ohmic losses in the telescope, spillover, blockage, and the radiation/attenuation of the atmosphere.

The following paragraphs describe the calibration procedure used at the 11m NRAO telescope as described by Ulich and Haas (1976).

The method of choice to calibrate mm-wavelength observations is to use a rotating chopper which alternately covers the feed horn with an ambient temperature microwave absorber. The method is attractive because it automatically compensates for changes in atmospheric absorption (Penzias and Burrus 1973).

The ambient temperature absorber is placed over the feed horn aperture and the antenna temperature measured is

$$T_{load} = G_s J(\nu_s, T_{amb}) + G_i J(\nu_i, T_{amb}) \quad (1)$$

where G is the gain in the receiver, T_{amb} is the ambient temperature of the absorber, the subscripts s and i indicate the signal and image sidebands, respectively, and

$$J(\nu, T) = \frac{h\nu/k}{\exp(h\nu/kT) - 1} \quad (2)$$

is the effective radiation temperature of a blackbody of temperature T at the frequency ν .

Note that the receiver amplifies not only the signal sideband but also the image sideband. The image sideband could be filtered out before the signal is amplified but this invariably involves the introduction of more noise at a crucial and sensitive point in the system.

Since this work is concerned primarily with detection and requires the most sensitive arrangement possible, the image rejection filter was not used. Consequently the following equations include terms for the image sideband as well as the signal sideband.

When the telescope is pointed at blank sky the antenna temperature is

$$T_{\text{sky}} = G_S [\eta_k J(\nu_S, T_S) + (1 - \eta_k) J(\nu_S, T_{\text{Sbr}})] \\ + \text{similar terms for the image sideband} \quad (3)$$

where η_k is the telescope efficiency considering spillover, blockage, and ohmic losses. The T_{Sbr} is the apparent brightness temperature from the spillover, blockage, and ohmic losses. The T_S and T_i (in the image sideband terms) are the brightness temperatures of the sky at the signal and image frequencies, respectively. They are given by

$$J(\nu_S, T_S) = J(\nu_S, T_m) [1 - \exp(-\tau_S A)] + J(\nu_S, T_{\text{bg}}) \exp(-\tau_S A) \quad (4)$$

and a similar image sideband equation. The T_m is the mean atmospheric temperature, T_{bg} is the brightness temperature of the cosmic background radiation, and τ_S and τ_i are the atmospheric zenith optical depths at the signal and image frequencies, A is the air mass in the observed direction.

The calibration signal is found by taking the difference between the load temperature and the antenna temperature looking at blank sky

$$\Delta T_{cal} = T_{load} - T_{sky} = G_S [J(\nu_S, T_{amb}) - \eta_L J(\nu_S, T_S) - (1 - \eta_L) J(\nu_S, T_{sbr})] + \text{similar image sideband terms} \quad (5)$$

When observing a spectral line source the antenna temperature is

$$T_{source} = G_S [\eta_L (1 - \eta_f) J(\nu_S, T_S) + \eta_L \eta_f \{ J(\nu_S, T_E) [1 - \exp(-\tau)] \exp(-\tau_S A) + J(\nu_S, T_{bg}) \exp(-\tau) \exp(-\tau_S A) + J(\nu_S, T_m) [1 - \exp(-\tau_S A)] \} + (1 - \eta_L) J(\nu_S, T_{sbr})] + \text{image terms for the sky brightness temperature} \quad (6)$$

and T_{sbr}

where T_E is the excitation temperature of the molecule, τ is the optical depth of the source, and η_f is the forward coupling efficiency given by

$$\eta_f = \frac{\iint_{\text{source}} P_n(\psi - \Omega) B_n(\psi) d\psi}{\iint_{2\pi} P_n(\Omega) d\Omega} \quad (7)$$

where P_n is the normalized antenna power pattern, B_n is the normalized apparent source brightness distribution, Ω is the direction of peak antenna gain, ψ is the direction of maximum source brightness, and $d\Omega$ and $d\psi$ are infinitesimal solid angles.

Essentially, η_f is the filling factor for the source within the telescope power pattern. If one observed an extended, uniformly bright source η_f would be 1. Otherwise it is less than 1 and dilutes the antenna temperature as is apparent from equation (8).

The difference in antenna temperature between the source and the sky is

$$\begin{aligned}\Delta T_{\text{source}} &\equiv T_{\text{source}} - T_{\text{sky}} \\ &= G_s \eta_L \eta_F \exp(-\tau_s A) (1 - e^{-\tau}) [J(\nu_s, T_E) - J(\nu_s, T_{bg})] \quad (8)\end{aligned}$$

The corrected antenna temperature of the source is defined as

$$T_A^* \equiv \Delta T_{\text{source}} / G_s \eta_L \exp(-\tau_s A) = \left(\frac{\Delta T_{\text{source}}}{\Delta T_{\text{cal}}} \right) T_C \quad (9)$$

where T_C is obviously

$$T_C \equiv \Delta T_{\text{cal}} / [G_s \eta_L \exp(-\tau_s A)] \quad (10)$$

Consequently

$$T_A^* = \eta_F (1 - e^{-\tau}) [J(\nu_s, T_E) - J(\nu_s, T_{bg})] \quad (11)$$

Note that several parameters do not appear, namely the receiver gain (G_s), atmospheric extinction $\exp(-\tau_s A)$, and antenna losses (η_L). These have been corrected for by an appropriate choice of T_C . From equation (9) it can be seen that we need only the ratio of the source temperature to the calibration temperature in addition to T_C to determine the source antenna temperature.

If we assume that the IF is small with respect to the LO frequency (a very safe assumption for this work) then $J(\nu_i, T) \sim J(\nu_s, T)$; that is, the signal and image temperatures are close enough to be considered equal then

$$\begin{aligned}
 T_c \sim & (1 + G_i/G_s)[J(\nu_s, T_m) - J(\nu_s, T_{bg})] \\
 & + (1 + G_i/G_s)[\exp(\tau_s A)][J(\nu_s, T_{sbr}) - J(\nu_s, T_m)] \\
 & + (G_i/G_s)\{\exp[(\tau_s - \tau_i)A] - 1\}[J(\nu_s, T_m) - J(\nu_s, T_{bg})] \\
 & + (1 + G_i/G_s)[\exp(\tau_s A)/\eta_\ell][J(\nu_s, T_{amb}) - J(\nu_s, T_{bg})] \quad (12)
 \end{aligned}$$

In general evaluation of this equation is difficult and an easier method is to use the definition of T_c [equation (10)]. Thus, only ΔT_{ca} , G_s , η_ℓ , and τ_s need to be measured as a function of elevation to determine T_c at a given frequency. Since the atmosphere changes little at high altitudes in the mm region, T_c is a constant function that varies slowly if at all with time.

By comparing equation (10) with equation (12), T_m (the mean atmospheric temperature) can be calculated. This is perhaps the most difficult value of equation (12) to determine. The others can be measured or estimated with reasonable confidence. Calibration for this work was done using equation (12) with the following values adopted:

$$G_s = G_i = 1$$

$$T_m = 280 \text{ K}$$

$$T_{bg} = 2.7 \text{ K}$$

$$T_{sbr} = 280 \text{ K}$$

$$T_{amb} = 290 \text{ K}$$

$$A = \sec (\text{zenith angle})$$

$$\eta_\ell = 0.87$$

$$\tau_i = 0.085$$

$$\tau_s = 0.35$$

APPENDIX II

THE PHYSICS OF CO SPECTRAL LINE CALCULATIONS

In this appendix the formation of CO line emission is treated. This is followed by consideration of column density calculations and the assumptions involved therein.

The one-dimensional time-independent equation of transfer is

$$\frac{dI_v}{ds} = -\kappa_v I_v + \epsilon_v \quad (1)$$

where κ_v is the volume absorption coefficient, ϵ_v is the volume emission coefficient, and I_v is the specific intensity at frequency v .

This can be integrated to give

$$I_v(s_0) = I_v(0)e^{-\tau_v(s_0)} + e^{-\tau_v(s_0)} \int_0^{s_0} \epsilon_v e^{\tau_v(s)} ds \quad (2)$$

where $\tau_v(s) = \int_0^s \kappa_v ds$ is the optical depth integrated along the line of sight from an initial point ($s = 0$) to the observer's position (s_0).

This can be further simplified by assuming the source is a uniform homogeneous cloud and that κ is due to an atomic or molecular transition. We now have

$$I_0(s_0) = I_0(0)e^{-\tau_0(s_0)} + \left(\frac{\epsilon_0}{\kappa_0}\right)(1 - e^{-\tau_0(s_0)}) \quad (3)$$

The first term is the attenuation of the background radiation as it passes through the cloud and the second term is the emission

by atoms or molecules in the cloud, corrected for self-absorption.

The quantity measured with a radio telescope is most closely related to the intensity at the transition frequency, $[I_o(s_o)]$ minus the intensity near the transition frequency $[I_v(s_o)]$. Since

$$I_v(s_o) \sim I_o(0)$$

$$\Delta I_o \equiv I_o(s_o) - I_o(0) = \left[\frac{\epsilon_o}{\kappa_o} - I_o(0) \right] (1 - e^{-\tau_o(s_o)}) \quad (4)$$

By convention radio astronomical measurements are usually made in temperature units and one can substitute the radiation temperature $[J(T_B) = c^2 I_v / 2k\nu^2]$ in the preceding equation. The brightness temperature is found from

$$I_v = B_v(T_B) = 2h\nu^3/c^2 (e^{h\nu/kT_B} - 1) \quad (5)$$

Obviously B_v is the Planck function and T_B is the temperature of the blackbody that subtends the same solid angle and emits the same specific intensity at ν . If the Rayleigh-Jeans limit ($h\nu/kT_B \ll 1$) applies then $J(T_B) \rightarrow T_B$. This is not always true for CO measurements.

The equation for the excess line temperature is then (Zuckerman and Palmer 1974)

$$\Delta J(T_{LE}) = J(T_L) - J(T_C) = [J(T_{ex}) - J(T_C)] (1 - e^{-\tau_\nu}) \quad (6)$$

where T_L is the line brightness temperature, T_C is the brightness temperature of the continuum, and T_{ex} is the excitation temperature of the molecule. Assuming local thermodynamic equilibrium (LTE) gives

a Boltzmann distribution of the rotational levels which can be written

$$\frac{n_u}{n_l} = \frac{g_u}{g_l} e^{-h\nu/kT_{ex}} \quad (7)$$

where n_u and n_l are the populations (cm^{-3}) in the upper and lower states, respectively, and g_u and g_l are the statistical weights of the levels.

Note that $\tau_\nu(s) = \int_0^s \kappa_\nu ds$ and (Lang 1974)

$$\kappa_\nu = \frac{c^2}{8\pi\nu^2} \frac{n_l}{\Delta\nu} \exp\left(\frac{h\nu}{kT_{ex}}\right) [1 - \exp\left(-\frac{h\nu}{kT_{ex}}\right)] A \quad (8)$$

where $\Delta\nu$ is the full-width at half-maximum for the line, T_{ex} is again the excitation temperature and the Einstein coefficient (A) for the spontaneous electric dipole transition is

$$A = \frac{64\pi^4\nu^3}{3hc^3} |\mu_J|^2 \quad (9)$$

where

$$|\mu_J|^2 = \mu^2 \frac{J(J+1)}{(2J+3)} \quad (10)$$

for the $J+1 \rightarrow J$ transition. Since $\mu = 0.112 \times 10^{-18}$ in cgs units, $|\mu_J|^2 = 5.02 \times 10^{-39}$ for the $J = 1 \rightarrow 0$ transition, $A = 8.9 \times 10^{-8} \text{ sec}^{-1}$.

Setting $N_l = \int_0^s n_l ds$ we can write

$$\tau_\nu(s) = \frac{c^2 A}{8\pi\nu^2} \frac{N_l}{\Delta\nu} \exp\left(\frac{h\nu}{kT_{ex}}\right) [1 - \exp\left(-\frac{h\nu}{kT_{ex}}\right)] \quad (11)$$

Substituting (7) into (11), assuming $h\nu \ll kT_{ex}$, and rearranging gives

$$N_u = \frac{8\pi\nu k}{hc^2 A} \int J_\nu(T_{\text{ex}}) \tau_\nu d\nu = \frac{8\pi\nu k}{hc^2 A} \int T_B d\nu \quad (12)$$

Since $T_A^* = \eta_f T_B$, the column density in the upper state (N_u) can now be found. To calculate the column density in all states one assumes LTE, then the number of molecules in the J state is given by (Herzberg 1950)

$$N_J = \frac{2J+1}{U} N_{\text{tot}} \exp\left(\frac{-hBJ(J+1)}{kT}\right) \quad (13)$$

where B is the rotational constant (5.764×10^{10} Hz for ^{12}CO) and U is the partition function

$$U = \sum_{J=0}^{\infty} (2J+1) \exp\left(\frac{-hBJ(J+1)}{kT}\right) \quad (14)$$

Table AII-1 gives values of U and $N_{\text{tot}}/N_{J=1}$ for several temperatures.

Table AII-1
Values of U and $N_{\text{tot}}/N_{J=1}$ for ^{12}CO

	$T_{\text{ex}} = 10 \text{ K}$	25	50	100	10^3
U	3.97	9.37	18.40	54.89	361.7
$N_{\text{tot}}/N_{J=1}$	2.30	3.90	6.85	19.34	121.1

Equation (12) and Table AII-1 can be used to find the total column density of CO under the various assumptions noted in the derivation. This estimate is a lower limit due to the assumption that $\tau_\nu \ll 1$; clearly, if the clouds are optically thick no information on column density is available.

Another line of reasoning can give space densities for a molecule if a few conditions are satisfied (see Rank et al. 1971 for a discussion). If a molecule is observed in emission, well-removed from discrete sources of radiation, it is likely that collisions raise T_{ex} well above T_R ($= 2.7$ K, the cosmic background radiation).

The relaxation rate between two molecular states for isotropic radiation is (Rank et al. 1971)

$$\frac{1}{\tau_r} = \frac{64\pi^4 v^3 |\mu|^2}{3hc^3 (1 - e^{-h\nu/kT_R})} \quad (15)$$

The collision rate can be written

$$\frac{1}{\tau_c} = \sum_m (n\sigma v)_m \quad (16)$$

where the summation is over all colliding species, n is the density of each species, σ is the effective cross-section, and v is the average relative velocity for the collisions. In most clouds the only particles abundant enough to contribute to equation (16) are atomic and molecular hydrogen.

Under these conditions the effective temperature of the radiation is

$$T_{\text{eff}} = \frac{\tau_r T_m + \tau_c T_R}{\tau_r + \tau_c} \quad (17)$$

where T_m is the temperature of the colliding particles. Since the molecule is seen in emission it follows that τ_c is not much larger than τ_r . The implication is that in order to see the molecule in

emission it must be elevated above T_R by some process (collisions in this case).

Thus, a minimum colliding particle density can be found by equating τ_r and τ_c . This gives

$$n = \frac{64\pi^4 |\mu|^2}{3h\lambda^3 \langle \sigma v \rangle (1 - e^{-h\nu/kT_R})} = \frac{A}{\langle \sigma v \rangle (1 - e^{-h\nu/kT_R})} \quad (18)$$

The usual approach to determine $\langle \sigma v \rangle$ is to use the geometric cross-section ($\sim 10^{-15} \text{ cm}^2$) and $v = 8kT_k/\pi m^{\frac{1}{2}} \sim 10^5 \text{ cm/sec}$ for $T_k = 100 \text{ K}$ and $m \equiv m(\text{H}_2)$. For CO this gives a minimum colliding particle density of $8.6 \times 10^2 \text{ cm}^{-3}$.

APPENDIX III

THE GEOMETRY IN AN INCLINED DISK

Projection effects serve to transform the desired quantities of circular velocity (v_c), azimuthal angle (θ), and radius (r) into their foreshortened counterparts, v_c' , θ' , and r' . In this appendix the relationships between these quantities are derived, also the calculation of the inclination is considered. The inclination angle is defined to be the angle between the plane of the disk and the plane of the sky.

Figure 24 illustrates the various parameters that will be used in the following material. The effect of inclination is to foreshorten, or project, the minor axis; the major axis is unaffected by this. The velocity component v_x (always perpendicular to the line of sight) is also unaffected by inclination, but it is not measurable. A component of v_y is observed as the radial velocity (v_r) and

$$v_r = v_y \sin i \quad (1)$$

The inclination angle is available, provided we know the true axial ratio (q) as well as the projected axial ratio (q'). Since $q' = b/a$, where b is the semi-minor axis and a is the semi-major axis as measured in the sky, and $\epsilon = (a - b)/a$ then

$$q' = 1 - \epsilon \quad (2)$$

The quantity q is calculated similarly, using the true axial ratio for

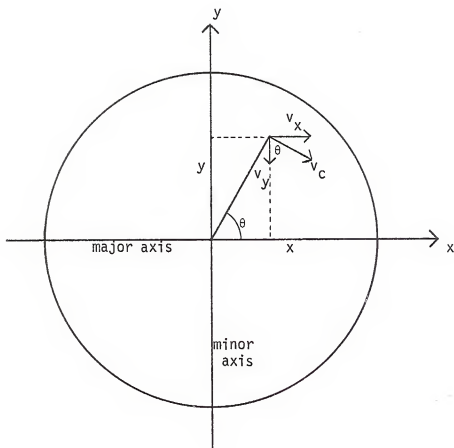


Figure 24. A disk system viewed face-on ($i = 0^\circ$). The x axis coincides with the major axis and the y axis is also the minor axis. The circular velocity, v_c , and its x and y components are indicated. Also shown is the azimuthal angle, θ .

the system. The inclination is then given by

$$\cos^2 i = \frac{q'^2 - q^2}{1 - q^2} \quad (3)$$

The true azimuthal angle, θ , is found from the projected angle, θ' , by

$$\tan \theta = \tan \theta' / \cos i \quad (4)$$

and v_r is related to v_c by

$$v_c = v_r / \cos \theta \sin i \quad (5)$$

Finally, the true radius of the point in question is given by

$$r = [x^2 + (y/\cos i)^2]^{\frac{1}{2}} \quad (6)$$

where x and y are the distances along the major and minor axes, respectively, and $y' = y/\cos i$.

Since the primed quantities can all be measured, the true values can be calculated using the relations given. The two assumptions made in the derivation are that the true axial ratio is known and that the figure of the system is an oblate ellipsoid supported by rotation about the minor axis.

REFERENCES

- Baan, W.A., Haschick, A.D., and Burke, B.F. 1978, Ap. J., 225, 339.
- Bailey, M.E. 1980, M.N.R.A.S., 191, 195.
- Balick, B., Faber, S.M., and Gallagher, J.S. 1976, Ap. J., 209, 710.
- Bautz, L.P. and Morgan, W.W. 1970, Ap. J. (Letters), 162, L149.
- Bertola, F. and Capaccioli, M. 1975, Ap. J., 200, 439.
- Binney, J. 1978, M.N.R.A.S., 183, 501.
- Blackman, R.B. and Tukey, J.W. 1958, "The Measurement of Power Spectra" (Dover: New York).
- Bottinelli, L. and Gouguenheim, L. 1977a, Astron. & Astrophys., 54, 641.
- Bottinelli, L. and Gouguenheim, L. 1977b, Astron. & Astrophys., 60, 223.
- Bottinelli, L. and Gouguenheim, L. 1979a, Astron. & Astrophys., 76, 176.
- Bottinelli, L. and Gouguenheim, L. 1979b, Astron. & Astrophys., 74, 172.
- Burstein, D. 1979a, Ap. J. Supplement, 41, 435.
- Burstein, D. 1979b, Ap. J., 234, 435.
- Burstein, D. 1979c, Ap. J., 234, 829.
- Butcher, H. and Oemler, A. 1978, Ap. J., 219, 18.
- Cheng, E.S., Saulson, P.R., Wilkinson, D.T., and Corey, B.E. 1979, Ap. J. (Letters), 232, L139.
- Coleman, G.D. and Worden, S.P. 1977, Ap. J., 218, 792.
- Cooper, B.F.C. 1976, in "Methods of Experimental Physics," 12 part B, ed. M.L. Meeks (Academic Press: New York), 280.
- de Vaucouleurs, G. 1959, Handbuch der Physik, 53, 275.

- de Vaucouleurs, G. 1977, in "The Evolution of Galaxies and Stellar Populations" (Yale University Observatory: New Haven), 74.
- de Vaucouleurs, G. and de Vaucouleurs, A. 1964, "Reference Catalog of Bright Galaxies" (University of Texas Press: Austin).
- de Vaucouleurs, G., de Vaucouleurs, A., and Corwin, H. 1976, "Second Reference Catalog of Bright Galaxies" (University of Texas Press: Austin).
- de Vaucouleurs, G. and Neito, J.-L. 1979, Ap. J., 230, 697.
- Dressler, A. 1980, Ap. J., 236, 351.
- Faber, S.M. and Gallagher, J.S. 1976, Ap. J., 204, 365.
- Faber, S.M. and Gallagher, J.S. 1979, Ann. Rev. Astron. & Astrophys., 17, 135.
- Faber, S.M. and Jackson, R. 1976, Ap. J., 204, 668.
- Field, G.B. 1975, in "Galaxies and the Universe," ed. A. Sandage, M. Sandage, and J. Kristian (Univ. of Chicago Press: Chicago).
- Ford, H.C., Jacoby, G., and Jenner, D.C. 1977, Ap. J., 213, 18.
- Ford, H.C. and Jenner, D.C. 1975, Ap. J., 202, 365.
- Ford, H.C., Jenner, D.C., and Epps, H.W. 1973, Ap. J. (Letters), 183, L73.
- Fosbury, R.A.E., Mebold, U., Goss, W.M., and Dopita, M.A. 1978, M.N.R.A.S., 183, 549.
- Gallagher, J.S., Faber, S.M., and Balick, B. 1975, Ap. J., 202, 7.
- Gallagher, J.S., Knapp, G.R., Faber, S.M., and Balick, B. 1977, Ap. J., 215, 463.
- Gallouet, L. and Heidmann, N. 1971, Astron. & Astrophys. Suppl., 3, 325.
- Gallouet, L., Heidmann, N., and Dampierre, F. 1973, Astron. & Astrophys. Suppl., 12, 89.
- Gallouet, L., Heidmann, N., and Dampierre, F. 1975, Astron. & Astrophys. Suppl., 19, 1.
- Giovanelli, R. 1979, Private communication.
- Gisler, G.R. 1976, Astron. & Astrophys., 51, 137.
- Gisler, G.R. 1979, Ap. J., 228, 385.

- Gisler, G.R. 1980, A. J., 85, 623.
- Gott, J.R. 1977, Ann. Rev. Astron. & Astrophys., 15, 235.
- Gottesman, S.T. and Weliachew, L. 1977, Ap. J., 211, 47.
- Graham, J.A. 1979, Ap. J., 232, 60.
- Gunn, J.E. and Gott, J.R. 1972, Ap. J., 176, 1.
- Gunn, J.E. and Oke, J.B. 1975, Ap. J., 195, 255.
- Guthrie, B.N.G. 1974, M.N.R.A.S., 168, 15.
- Hausman, M.A. and Ostriker, J.P. 1978, Ap. J., 224, 320.
- Haynes, M.P., Brown, R.L., and Roberts, M.S. 1978, Ap. J., 221, 414.
- Haynes, M.P. and Roberts, M.S. 1979, Ap. J., 337, 767.
- Herbig, G.H. 1970, "Proc. of the XVIIth Liège Symposium," 59, 13.
- Herzberg, G. 1950, "Spectra of Diatomic Molecules" (Van Nostrand: New York), 125.
- Hodge, P.W. 1963, A. J., 68, 691.
- Hodge, P.W. 1973, Ap. J., 182, 671.
- Hubble, E.P. 1926, Ap. J., 64, 321.
- Hubble, E.P. 1936, "The Realm of the Nebulae" (Yale University Press: New Haven), 36.
- Huchtmeier, W.K., Tammann, G.A., and Wendker, H.J. 1977. Astron. & Astrophys., 57, 313.
- Hulsbosch, A. 1980, Private communication.
- Humason, M.L., Mayall, N.U., and Sandage, A.R. 1956, A. J., 61, 97.
- Illingworth, G. 1977, Ap. J. (Letters), 218, L43.
- Johnson, H.E. and Axford, W.I. 1971, Ap. J., 165, 381.
- Jones, B.T. 1976, Rev. Mod. Phys., 48, 107.
- Jura, M. 1977, Ap. J., 212, 634.
- Kent, S.M. and Sargent, W.L.W. 1979, Ap. J., 230, 667.
- Killian, D.J. 1978, Ph.D. Dissertation, University of Florida.

- Knapp, G.R., Faber, S.M., and Gallagher, J.S. 1978a, A. J., 83, 11.
- Knapp, G.R., Gallagher, J.S., and Faber, S.M. 1978b, A. J., 83, 139.
- Knapp, G.R. and Jura, M. 1976, Ap. J., 209, 782.
- Knapp, G.R., Kerr, F.J., and Williams, B.A. 1978c, Ap. J., 222, 800.
- Lang, K.R. 1974, "Astrophysical Formulae" (Springer-Verlag: New York), 161.
- Larson, R.B. 1974, M.N.R.A.S., 169, 229.
- Larson, R.B. and Tinsley, B.M. 1974, Ap. J., 192, 293.
- Larson, R.B. and Tinsley, B.M. 1978, Ap. J., 219, 46.
- Lea, S.M. and De Young, D.S. 1976, Ap. J., 210, 647.
- Lo, K.Y. and Sargent, W.L.W. 1979, Ap. J., 227, 756.
- Lucas, R. 1974, Astron. & Astrophys., 36, 465.
- Lynden-Bell, D. 1967, M.N.R.A.S., 136, 101.
- Martin, R.N. and Barrett, A.H. 1978, Ap. J. Suppl., 36, 1.
- Mathews, W.G. and Baker, J.C. 1971, Ap. J., 170, 241.
- Mathewson, D.S., Cleary, M.N., and Murray, J.D. 1974, Ap. J., 190, 291.
- Mathewson, D.S., Cleary, M.N., and Murray, J.D. 1975, Ap. J. (Letters), 195, L97.
- McHardy, I.M. 1974, M.N.R.A.S., 169, 522.
- Mezger, P.G. and Smith, L.F. 1977, in "Star Formation, I.A.U. Symp. No. 75," ed. T. de Jong and A. Maeder (D. Reidel: Dordrecht), 133.
- Morgan, W.W. 1958, Pub. A.S.P., 70, 364.
- Morgan, W.W. 1959, Pub. A.S.P., 71, 394.
- Morton, D.C. 1975, Ap. J., 197, 85.
- Oemler, A. 1974, Ap. J., 194, 1.
- Oemler, A. 1977, Highlights of Astronomy, 4, 253.
- Osterbrock, D. 1960, Ap. J., 132, 325.

- Osterbrock, D. 1962, in "Interstellar Matter in Galaxies" (Benjamin: New York), 111.
- Ostriker, J.P. 1977, in "The Evolution of Galaxies and Stellar Populations," ed. B.M. Tinsley and R.B. Larson (Yale University Observatory: New Haven), 369.
- Ostriker, J.P. and Hausman, M.A. 1977, Ap. J. (Letters), 217, L125.
- Ostriker, J.P. and Tremaine, S.D. 1975, Ap. J. (Letters), 202, L113.
- Penzias, A.A. and Burrus, C.A. 1973, Ann. Rev. Astron. & Astrophys., 11, 51.
- Peterson, C.J. 1978, Ap. J., 222, 81.
- Rank, D.M., Townes, C.H., and Welch, W.J. 1971, Science, 174, 1083.
- Reif, K., Mebold, U., and Goss, W.M. 1978, Astron. & Astrophys., 67, L1.
- Rickard, L.J., Palmer, P., Morris, M., Turner, B.E., and Zuckerman, B. 1977, Ap. J., 213, 673.
- Riley, J.M. 1975, M.N.R.A.S., 170, 53.
- Roberts, M.S. and Steigerwald, D.G. 1977, Ap. J., 217, 883.
- Rood, H. 1979, Ap. J., 232, 699.
- Rowan-Robinson, M. 1979, Ap. J., 234, 111.
- Rubin, V.C., Ford, W.K., Peterson, C.J., and Oort, J.H. 1977, Ap. J., 211, 693.
- Sandage, A.R. 1961, "The Hubble Atlas of Galaxies" (Carnegie Inst. of Washington: Washington).
- Sargent, W.L.W., Young, P.J., Boksenberg, A., Shortridge, K., Lynds, C.R., and Hartwick, F.D.A. 1978, Ap. J., 221, 731.
- Schechter, P.L. and Gunn, J.E. 1979, Ap. J., 229, 472.
- Schneps, M.H., Ho, P.T.P., Barrett, A.H., Buxton, R.B., and Myers, P.C. 1978, Ap. J., 225, 808.
- Shane, W.W. 1980, Astron. & Astrophys., 82, 314.
- Shostak, G.S. 1978, Astron. & Astrophys., 54, 919.
- Silk, J. and Norman, C. 1979, Ap. J., 234, 86.
- Smoot, G.F. and Lubin, P.M. 1979, Ap. J. (Letters), 234, L83.

- Sunyaev, R.A. 1977, in "Radio Astronomy and Cosmology, I.A.U. Symp. No. 74," ed. D.L. Jauncey (D. Reidel: Dordrecht).
- Tammann, G.A. 1974, in "Supernovae and Supernovae Remnants," ed. C.B. Cosmovici (D. Reidel: Dordrecht).
- Tartar, J. 1975, Ph.D. Dissertation, University of California, Berkeley.
- Tytler, D. and Vidal, N. 1978, M.N.R.A.S., 182, 33p.
- Ulich, B.L. and Haas, R.W. 1976, Ap. J. Suppl., 30, 247.
- Unwin, S.C. 1980, M.N.R.A.S., 190, 551.
- van den Bergh, S. 1960a, Ap. J., 131, 215.
- van den Bergh, S. 1960b, Ap. J., 131, 558.
- van den Bergh, S. 1975, Ann. Rev. Astron. & Astrophys., 13, 217.
- van den Bergh, S. 1976a, Ap. J., 208, 673.
- van den Bergh, S. 1976b, Ap. J., 206, 883.
- van den Bergh, S. 1976c, A. J., 81, 797.
- White, S. 1976, M.N.R.A.S., 174, 19.
- Wright, M.C.H. 1974, in "Galactic and Extra-Galactic Radio Astronomy," ed. G.L. Verschuur and K.I. Kellerman (Springer-Verlag: New York), 291.
- Young, P.J., Bokseberg, A., Lynds, C.R., and Hartwick, F.D.A. 1978a, Ap. J., 222, 450.
- Young, P.J., Sargent, W.L.W., Kristian, J., and Westphal, J.A. 1979, Ap. J., 234, 76.
- Young, P.J., Westphal, J.A., Kristian, J., Wilson, C.P., and Landauer, F.P. 1978b, Ap. J., 221, 721.
- Zuckerman, B. and Palmer, P. 1974, Ann. Rev. Astron. & Astrophys., 12, 279.

BIOGRAPHICAL SKETCH

On reaching the age of 13, Douglas William Johnson had managed to take apart every watch, toaster, alarm clock, and gadget in his parents' wood frame home in both Gas City, Indiana, and Connellesville, Pennsylvania. His sisters, Rhonda and Peggy, grew up with the enduring fear their hair dryer would fall prey to his eager little hands.

Doug's mother comforted herself with the conviction that her second eldest son would go on to become a mechanic. Anyone who so loved to work with his hands, she reasoned, must be born to things mechanical.

Mary Ann Johnson's instincts about her son were good, but she had not reckoned on the draw of the night sky. Those brilliant, changing lights--completely out of reach--caught Doug's interest effortlessly. When his father's job as a Postal Inspector brought the family east to New Jersey, in 1968, the would-be astronomer constructed his own telescope to ply his trade in the Johnson's lush and overgrown backyard. Doug attended Boonton High School and pursued his favorite subjects of physics and math.

With a well-nurtured respect for the universe and the deep curiosity of a scientist, Doug went on to college at Rensselaer Polytechnic Institute in Troy, New York. In 1975, equipped with a bachelor's degree in physics, and a wife gracious enough to work full-time, he arrived in Gainesville. It was late summer, a time designed to kill Yankees with

its stifling, muggy heat. But the Johnsons survived and prospered, spreading their prosperity among the animal kingdom through the addition of four highly personable cats and a sweet-faced mongrel from the county pound to their family.

When lured away from his computers, mounds of graph paper, or blackboards, Doug holds true to his earliest love of tinkering. He is an accomplished carpenter, a competent mechanic, and makes a mean pitcher of frozen daquiris.

Though not given over to an abandoned social life, he misses few science fiction movies. His friends are a peculiar mixture of astronomy graduate students and newspaper types--a situation forced on him by his wife, Maryfran, the tolerant breadwinner of the family for the last five years.

I certify that I have read this study and that in my opinion it conforms to acceptable standards of scholarly presentation and is fully adequate, in scope and quality, as a dissertation for the degree of Doctor of Philosophy.

Stephen T. Gottesman

Dr. Stephen T. Gottesman, Chairman
Associate Professor of Astronomy

I certify that I have read this study and that in my opinion it conforms to acceptable standards of scholarly presentation and is fully adequate, in scope and quality, as a dissertation for the degree of Doctor of Philosophy.

J. D. Hunter for T. D. Carr

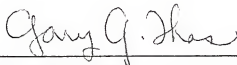
Dr. Thomas D. Carr
Professor of Astronomy

I certify that I have read this study and that in my opinion it conforms to acceptable standards of scholarly presentation and is fully adequate, in scope and quality, as a dissertation for the degree of Doctor of Philosophy.

Kwan-Yu Chen

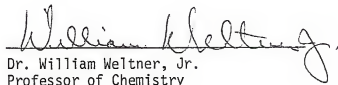
Dr. Kwan-Yu Chen
Professor of Astronomy

I certify that I have read this study and that in my opinion it conforms to acceptable standards of scholarly presentation and is fully adequate, in scope and quality, as a dissertation for the degree of Doctor of Philosophy.



Dr. Gary G. Ihas
Associate Professor of Physics

I certify that I have read this study and that in my opinion it conforms to acceptable standards of scholarly presentation and is fully adequate, in scope and quality, as a dissertation for the degree of Doctor of Philosophy.



Dr. William Weltner, Jr.
Professor of Chemistry

This dissertation was submitted to the Graduate Faculty of the Department of Astronomy in the College of Liberal Arts and Sciences and to the Graduate Council, and was accepted as partial fulfillment of the requirements for the degree of Doctor of Philosophy.

August 1980

Dean, Graduate School